A DYNAMIC FINITE ELEMENT MODEL FOR HIGH SPEED CRACK PROPAGATION ANALYSIS

A Thesis Submitted
in Partial Fulfillment of the Requirements
for the Degree of

MASTER OF TECHNOLOGY

February, 2000

by

GIRISH V DESHMUKH

DEPARTMENT OF MECHANICAL ENGINEERING
INDIAN INSTITUTE OF TECHNOLOGY
KANPUR – 208016 (INDIA)

CERTIFICATE

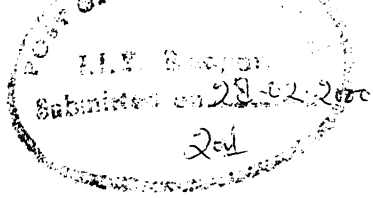

It is certified that the work contained in the thesis entitled, "A DYNAMIC FINITE ELEMENT MODEL FOR HIGH SPEED CRACK PROPAGATION ANALYSIS" by *Mr. Girish V Deshmukh* has been carried out under my supervision and that this work has not been submitted elsewhere for a degree.

N N Kishore

Dr. N. N. Kishore
Professor,
Department of Mechanical Engg,
Indian Institute of Technology,
Kanpur.

February, 2000

Dedicated to

MY PARENTS

Contents

ACKOWLEDGEMENTS

At the outset, I wish to express my deep sense of gratitude and indebtedness towards Dr. N N Kishore for his inspiring guidance, invaluable suggestions and constructive criticism. He was always a great source of encouragement throughout my thesis work. I am highly indebted to him for the expertise and guidance I received from him while working on this thesis and throughout my Mtech program. It is his generosity and kind nature besides technical expertise, which makes him venerable to me.

I would like to thank all my friends in Hall V for their cooperation. I would like to thank all the members of *ghatmandal* for their support and encouragement and for making my stay in IITK memorable and enjoyable. Names that can't go unmentioned are Abhi, Amod and Yogesh who were of great help to me throughout my MTech program.

Girish V Deshmukh

ABSTRACT

In dynamic fracture problem role of material inertia becomes significant. The formulation and analytical solution of dynamic fracture problem are of very complex nature. Experimental and numerical methods like finite element method are used extensively for solving dynamic fracture problem. Existing methods for simulating crack phenomenon in dynamic fracture problems have certain drawbacks such as , they are either computationally very intensive or give oscillations in the solution.

In this work, a model is proposed for simulating dynamic crack propagation phenomenon in finite element method. Gradual propagation of crack from one node to the next node is simulated by adding a 1-D elastic element at the crack tip node, whose stiffness value is reduced gradually to zero as the crack propagate in the element. Shape function for elemental mass matrix is modified so that the mass of the element surrounding the crack tip also varies as a function of crack length within the element, starting from zero to the value corresponding to regular shape function.

The finite element model is first validated with hypothetical data for different crack speeds. Results give smooth variation of energy release rate curve for various crack velocities. This method is also applied to determine the dynamic G_I for the experimental data on glass fabric/epoxy composites. Results show that the energy release rate gives fairly smooth variation and stable solution

List of Figures

List of Tables

LIST OF SYMBOLS

a	Non dimensional crack length
a′	Crack length
A	Crack surface area
B	Thickness of the specimen
[B]	Elastic strain displacement matrix
c	Dilatation wave velocity
C,C_1,C_2	Constants in stiffness release formulation
[D]	Elastic constitutive relation matrix
E	Young's modulus of elasticity
F_{HB}	Holding back force at crack tip
$\{F\}$	Global load vector
G	Energy release rate
G_{ini}	Initiation toughness
G_{prop}	Propagation toughness
K_s	Spring stiffness at the crack tip
K_0	Static stiffness at the crack tip
k_d	Damping coefficient
$[K]$	Global stiffness matrix
$[K']$	Effective global stiffness matrix
L	Length of specimen
$[M]$	Global mass matrix
N_E	Number of elements
$[N]$	Matrix of interpolation function

$\{\dot{q}\}$	Velocity component
$\{\ddot{q}\}$	Acceleration component
Δt	Time step
T	Kinetic energy
T_{ini}	Initiation toughness
u_0	Displacement of node when crack tip reaches the next node and element opens up completely.
U	Strain energy in body
{u}	Displacement vector
V_c	Crack velocity
W_{ext}	Work done due to external forces
W	Width of specimen
ξ, η	Natural coordinates
Π	Total potential energy
ρ	Density of material
υ	Poisson ratio
$\{\delta q\}$	Virtual displacements
$\{\delta\varepsilon\}$	Virtual strains
$\{\sigma\}$	Stress component

CHAPTER 1

INTRODUCTION

1.1 Introduction

Despite the development in many fields of fracture mechanics and its numerous applications, formulation and analytical solution of dynamic problem of this theory remained unexplored, until recently, on account of their extremely intricate nature. A large number of problems still remain unsolved in the description of this process on microscopic and macroscopic levels.

Time dependent applied load may arise by vibration of structure or unbalance in the machine, wave impact, seismic distribution etc. These kinds of problems are often solved by neglecting time dependence and are solved under static or quasi-static conditions. Quasi-static mechanics of brittle fracture render only first approximation to the description of fracture and can simply indicate whether or not catastrophic growth of crack sets in.

Structural members that are subjected to cyclic loading such as vibrations, microscopic imperfections in the material give rise to microscopic cracks, which in turn grow into crack of significant size over a passage of time. At this stage further growth of crack in a stable or unstable manner depends not only on the material but also on the nature of loading i.e. static or dynamic. An understanding of the mechanics of dynamic fracture is necessary for developing sound design methodologies.

1.2 Mechanics of Dynamic Fracture

Subject of dynamic fracture can be broadly described as that of mechanics of solids, containing stationary or propagating cracks, wherein effect of material inertia and stress wave interaction play significant role.

Inertia effect can arise, either from rapidly applied loading on the cracked body or from rapid crack propagation. In case of rapid loading, influence of load is transferred to the crack by means of stress wave through the material. In case of rapid crack propagation material particles on the opposite crack faces displace with respect to each other.

As per the guidelines given by Freund [1], in former case, inertia effect will be significant if the characteristic time (i.e. maximum load by rate of load increase) is larger than time required for stress wave to travel at the characteristic wave speed of the material over a representative length of the body (crack length or distance from crack edge to the loaded boundary).

Fundamental framework of dynamic fracture mechanics relies primarily on solution for dynamic behaviour of solid containing crack. These solutions are characterised by

i) Stress wave integration
ii) Need to take into account kinetic energy in the global energy balance of the fracturing body
iii) Inertia effect of the material

One logical way of classifying dynamic fracture problem is as follows (Nishioka and Atluri[2])

i) Solids containing stationary cracks subjected to dynamic loading
ii) Solids containing dynamically propagating cracks under quasi-static loading
iii) Solids containing dynamically propagating cracks under dynamic loading

Analytical solutions to the dynamic fracture problem for some cases are available. However, these solutions are limited to cases of simple loading and of unbounded plane bodies. However, the interaction of stress waves emanating from the crack tip or those reflected from the boundaries make closed form solution of dynamic problem intractable and it becomes mandatory to analyse such problem using computational methods.

Even laboratory evaluation of dynamic fracture toughness is based on the measurement of instantaneous dynamic stress field close to the propagating crack tip. Such direct measurements are difficult and require sophisticated instruments and accurate measurements. To overcome these difficulties, hybrid experimental and numerical methods are often preferred. This is one of the reasons for the advancement of the state of science of dynamic fracture mechanics relies heavily on the simultaneous advancement in computational methods.

1.3 Literature Survey

Though considerable amount of work has been done to study the fracture phenomena through numerical methods, only rectangular double cantilever beam (DCB) specimens were given special interest. Owen and Shantaram [3] started the case of finite element method to study dynamic crack growth. They studied DCB specimen and pipeline problem under transient loading. The crack was advanced from one node to the next node and when stress at the gauss point nearest to the crack tip exceeded a certain value, damping coefficient was made zero at the released node. The crack propagation history was simulated for the given loading conditions.

Nishioka and Atluri [4] investigated the crack propagation and arrest in high strength steel DCB specimen using moving singular dynamic finite element procedure. An edge crack in a rectangular DCB specimen was propagated by

procedure. An edge crack in a rectangular DCB specimen was propagated by inserting a wedge and the results were compared with experimental data. In another work, Nishioka and Atluri [5] presented the results of generation and prediction studies of dynamic crack propagation in plane stress and plane strain cases. The studies were conducted by using FEM, taking into account stress singularity near the crack tip. Variation of dynamic stress intensity factor with time and variation of dynamic fracture toughness with velocity were studied and compared with available experimental results.

Nishioka and Atluri [2] gave elaborate information on the analysis of dynamic fracture using FEM. The most common ways to deal with the crack tip region was to simulate crack growth through gradual release of elemental nodal forces or embedding a moving element in which interpolation functions are determined by the continuum near tip fields at the crack tip in the mesh, and J-Integral consideration. Following special description the differential equation in time for the node point variables must be integrated. Because the dynamic fields associated with rapid crack growth are rich in high frequency content, small time steps are required for accuracy. Because of natural restriction to small time steps, the author's report that many times combination of conditionally stable explicit time integration scheme and diagonalised mass matrix are found to be accurate.

Chiang [6] presented a numerical procedure based on eigen function to determine the dynamic stress intensity factor for a crack moving at steady state under antiplane strain condition. An edge crack problem and a radial crack problem were solved using traction and displacement boundary conditions separately. It was shown that the dynamic effect was relatively insignificant for low crack propagation speeds provided that specimen size was fairly large.

Thesken and Gudmundson [7] worked with elasto-dynamic moving element formulation incorporating a variable order singular element to enhance the local crack tip description. Kennedy and Kim [8] incorporated micropolar elasticity theory into a plane strain finite element formulation to analyse the dynamic response of the crack.

Materials with strong micropolar properties were found to have significantly lower dynamic energy release rate than their classical material counterparts. Wang and Williams [9] investigated high-speed crack growth in a thin double cantilever beam specimen using FEM. The cantilever end was loaded under an initial step displacement of 1mm and then pulled with a constant velocity the crack was propagated at assumed speed by gradual node release technique. Large dynamic effects were observed because of wave reflections within finite specimen size. The reflection and interaction of the waves from free boundary were avoided by limiting the duration of study. Beissel, Johnson and Popelar [10] presented an algorithm, which allows crack propagation in any direction but doesn't require remeshing or the definition of new contact surfaces. This is achieved by tracking the path of the crack tip and failing the element crossed by the path such that they can no longer sustain tensile volumetric stress. The edges of these failed elements simulate crack faces that can sustain only compressive normal traction. Lin and Smith[11] presented a method wherein crack growth is predicted in a step by step basis from Paris law using stress intensity factor calculated by using finite element method. The crack front is defined by a cubic spline curve from a set of nodes. Both the one quarter node crack opening and 3-D J-Integral method are used to calculate stress intensity factor. Automatic remeshing of finite element model to a new position that defines the new crack front enables the crack propagation to be followed.

1.4 Present Work

Present work is a modification of 'Stiffness Release Model' for dynamic crack propagation in DCB specimen(Siva Reddy [12]). In the 'Stiffness Release Model', instead of reducing crack tip nodal force as is done in force release models, an

additional one dimensional elastic element is attached at the crack tip node whose stiffness value is gradually reduced, as the crack advance from one node to next node.

In the present work, stiffness release model is further improved and the mass of the element surrounding the crack tip is modified as the crack propagates and the effect of various other parameters with crack velocity is also studied.

Chapter 2 describes the basics of FEM formulation and the existing propagation model.

Chapter 3 presents the crack propagation element model.

Chapter 4 describes the results and discussion.

Chapter 5 presents the conclusion of the present work and scope of future work.

CHAPTER 2

BASICS OF FEM AND EXISTING CRACK PROPAGATION MODELS

2.1 FEM Formulation

2.1.1 FEM Equation

Equations that govern the dynamic response of a structure are derived by using virtual work principle involving work of external forces, internal, inertial and viscous forces for any small admissible motion.

The finite element solution involves discretization of domain (Ω) into suitable elements and approximating the field variable interior to the element in terms of nodal values using suitable shape function.

FEM equations can be derived from the virtual equation for the body as

$$\int_{\Omega}\{\delta\varepsilon\}^{T}\{\sigma\}dV+\int_{\Omega}\{\delta q\}^{T}\rho\{\ddot{q}\}dV+\int_{\Omega}\{\delta q\}^{T}k_{d}\{\dot{q}\}dV \qquad (2.1)$$
$$=\int_{\Omega}\{\delta q\}^{T}\{P_{B}\}dV+\int_{\Gamma_{\sigma}}\{\delta q\}^{T}\{P_{s}\}dS$$

where

$\{\delta q\},\{\delta\varepsilon\}$: Virtual displacements and corresponding strains

$\{\dot{q}\},\{\ddot{q}\}$: Velocity and acceleration component

$\{\sigma\}$: Stress component

ρ : Material density

k_d : Damping coefficient

$\{P_B\}$: Body forces

$\{P_s\}$: Surface traction

Γ_σ : Surface traction boundary

Displacement $\{q\}^{(e)}$ within element can be expressed in terms of its nodal values $\{Q\}^{(e)}$ as

$$\{q\}^{(e)} = [N]^{(e)}\{Q\}^{(e)} \tag{2.2}$$

Strain-displacement relation can be written as

$$\{\varepsilon\}^{(e)} = [B]^{(e)}\{Q\}^{(e)} \tag{2.3}$$

Stress-strain relation or constitutive equation is given as

$$\{\sigma\}^{(e)} = [D]^{(e)}\{\varepsilon\}^{(e)} = [D]^{(e)}[B]^{(e)}\{Q\}^{(e)} \tag{2.4}$$

where,

$[N]^{(e)}$ - Matrix of shape function

$[B]^{(e)}$ - Strain displacement matrix

$[D]^{(e)}$ - Matrix of material properties

The present analysis is made for an undamped system and neglecting body forces. The stresses, strains and displacements are expressed in terms of nodal variables as given in equations 2.2, 2.3 and 2.4. This on substitution in Eqn (2.1) gives,

$$\{\delta q\}^T\left[\sum_{e=1}^{N_E}\left(\int_{\Omega^{(e)}}[B]^{(e)^T}[D]^{(e)}[B]^{(e)}dv\right)\{q\}+\sum_{e=1}^{N_E}\left(\int_{\Omega^{(e)}}\left(\rho[N]^{(e)^T}[N]^{(e)}dv\right)\right)\{\ddot{q}\}-\sum_{e=1}^{N_E}\left(\int_{T_\sigma^{(e)}}[N]^{(e)^T}\{P_s\}^{(e)}dv\right)\right]=0 \tag{2.5}$$

where summation is over all elements, N_E.

since $\{\delta q\}$ is taken arbitrary, satisfying kinematic conditions, the equation can be written as,

$$\sum_{e=1}^{N_E}\left(\int_{\Omega^{(e)}}[B]^{(e)T}[D]^{(e)}[B]^{(e)}|J|d\xi d\eta\right)\{q\}+\sum_{e=1}^{N_E}\left(\int_{\Omega^{(e)}}\rho[N]^{(e)T}[N]^{(e)}|J|d\xi d\eta\right)\{\ddot{q}\} \qquad (2.6)$$

$$=\sum_{e=1}^{N_E}\left(\int_{\Gamma_\sigma^{(e)}}[N]^{(e)T}\{P_s\}^{(e)}|J|d\xi d\eta\right)$$

The final set of assembled equations can be written as,

$$[K]\{Q\}+[M]\{\ddot{Q}\}=\{F\} \qquad (2.7)$$

where

$[M]=\sum[M]^{(e)}$, Global mass matrix

$[K]=\sum[K]^{(e)}$, Global stiffness matrix

$\{F\}=\sum\{F\}^{(e)}$, Global applied force vector

and

$$[K]^{(e)}=\int_{\Omega^{(e)}}[B]^{(e)T}[D]^{(e)}[B]^{(e)}|J|d\xi d\eta \text{ , Elemental stiffness matrix}$$

$$[M]^{(e)}=\int_{\Omega^{(e)}}\rho[N]^{(e)T}[N]^{(e)}|J|d\xi d\eta \text{ , Elemental mass matrix} \qquad (2.8)$$

$$\{F\}^{(e)}=\int_{\Gamma^{(e)}}[N]^{(e)T}\{P_S\}^{e}|J|d\xi \text{ , Elemental force vector}$$

2.1.2 Integration algorithm

Equations of equilibrium governing linear dynamic response of a system of finite element is given by Eqn (2.7).

Eqn 2.7 can be written as,

$$F_I(t) + F_E(t) = F(t) \qquad \textbf{(2. 9)}$$

where, $F_I(t)$ are inertia forces, $F_I(t) = [M]\{\ddot{Q}\}$, $F_E(t)$ are elastic forces , $F_E(t) = [K]\{Q\}$, all of them being time dependent. Thus, in dynamic analysis, the displacements $\{Q\},\{\varepsilon\}$ and {F} are all functions of time.

Mathematically, for small deformation Δt can be assumed. Eqn (2.7) represent a system of linear differential equation of second order and the solution to the equation can be obtained by standard procedures of solving differential equations.

The procedures for solving differential equations are divided into direct integration and mode superposition of which former is preferred in wave propagation problem. In this integration scheme, there are many different methods, which can be classified as 'Explicit' or 'Implicit' whose advantages and disadvantages are given by Bathe[13].

In the present work two different integration schemes are used

1. Newmark's method
2. θ – Method

which are discussed in the following Section.

2.1.2.1 Newmark's Method of Integration

Newmark's method is an extension of 'Linear acceleration method', in which, linear variation of acceleration is assumed from time t to $t + \Delta t$.

Velocity and acceleration approximated in terms of displacements are

$$^{t+\Delta t}\{\dot{q}\} = {}^{t}\{\dot{q}\} + \left[(1-\delta)\,{}^{t}\{\ddot{q}\} + \delta\,{}^{t+\Delta t}\{\ddot{q}\}\right]\Delta t \qquad \textbf{(2. 10)}$$

$$ {}^{t+\Delta t}\{q\} = {}^{t}\{q\} + {}^{t}\{\dot{q}\}\Delta t + \left[\left(\frac{1}{2}-\alpha\right){}^{t}\{\ddot{q}\} + \delta\, {}^{t+\Delta t}\{\ddot{q}\}\right]\Delta t^2 \qquad \textbf{(2. 11)} $$

where α and δ are the parameters chosen suitably to have accuracy and stability. Usually, α and δ are taken as 0.25 and 0.5 respectively to get unconditional stability. As mentioned earlier, equilibrium at $t+\Delta t$ is considered along with these approximations. Solving equations 2.8 and 2.9,we get expressions for ${}^{t+\Delta t}\{\dot{q}\}$ and ${}^{t+\Delta t}\{\ddot{q}\}$, in terms unknown displacement ${}^{t+\Delta t}\{q\}$. These are then substituted in the following equation to solve for ${}^{t+\Delta t}\{q\}$.

$$ [M]{}^{t+\Delta t}\{\ddot{q}\} + [K]{}^{t+\Delta t}\{q\} = {}^{t+\Delta t}\{F\} \qquad \textbf{(2. 12)} $$

Entire method can be summarised as follows. (Bathe [13])

1. Form global stiffness matrix [K], and mass matrix [M].

2. Initialise ${}^{0}\{q\}, {}^{0}\{\dot{q}\}, {}^{0}\{\ddot{q}\}$.

3. Select time step Δt and calculate integration constants

$$ a_0 = \frac{1}{\alpha\Delta t^2} \;;\; a_1 = \frac{\delta}{\alpha\Delta t} \;;\; a_2 = \frac{1}{\alpha\Delta t} \;;\; a_3 = \frac{1}{2\alpha} - 1 \qquad \textbf{(2. 13)} $$

$$ a_4 = \frac{\delta}{\alpha} - 1 \;;\; a_5 = \frac{\Delta t}{2}\left(\frac{\delta}{\alpha} - 2\right) \;;\; a_6 = \Delta t(1-\delta) \;;\; a_7 = \delta\Delta t $$

For effective stiffness, $[K'] = [K] + a_0[M]$ **(2. 14)**

4. For each time step :

   (i) Calculate effective load at $t+\Delta t$

$$ {}^{t+\Delta t}\{F'\} = {}^{t+\Delta t}\{F\} + [M]\left(a_0^t\{q\} + a_2^t\{\dot{q}\} + a_3^t\{\ddot{q}\}\right) \qquad \textbf{(2. 15)} $$

(ii) Solve for displacement at time $t+\Delta t$ by $[K']^{t+\Delta t}\{q\}={}^{t+\Delta t}\{F'\}$

(iii) Calculate acceleration and velocity at time $t+\Delta t$

$$ {}^{t+\Delta t}\{\ddot{q}\} = a_0\left({}^{t+\Delta t}\{q\} - {}^{t}\{q\}\right) - a_2^t\{\dot{q}\} - a_3^t\{\ddot{q}\} \qquad (2.16) $$

$$ {}^{t+\Delta t}\{\dot{q}\} = {}^{t}\{\dot{q}\} + a_6^t\{\ddot{q}\} + a_7^{t+\Delta t}\{\ddot{q}\} $$

2.1.2.2 θ -Method

Hoff and Pahl[14] presented an unconditionally stable second-order-accurate θ method. This method is found to be more stable compared to Newmark's method as also will be shown later.

θ – method can be summarised in brief as follows.

1. Choose parameters θ_1 (0.95 to 1.0) and θ_0 (1.0)

2. Form global stiffness matrix [K], and mass matrix [M].

3. Initialise ${}^0\{q\}, {}^0\{\dot{q}\}, {}^0\{\ddot{q}\}$.

4. Select time step Δt and calculate integration constants

$$ a_0 = \frac{4.0\times\theta_1^2}{\Delta t^2} \; ; \; a_1 = \frac{(1.5-\theta_1)\times 4.0\times\theta_1^2}{\Delta t} \; ; \qquad (2.17) $$

For effective stiffness, $[K'] = [K] + a_0[M]$ (2.18)

5. For each time step :

(iv) Calculate effective load at $t+\Delta t$

$$ {}^{t+\Delta t}\{F'\} = {}^{t+\Delta t}\{F\} + [M]\left(a_0^t\left(\{q\} + \Delta t\{\dot{q}\} + 0.5\times\Delta t^2\{\ddot{q}\}\right) - \{\ddot{q}\}\right) \qquad (2.19) $$

$$ + (1.0-\theta_1)\Delta t\{\dot{q}\}^{t-\Delta t} $$

(v) Solve for displacement at time $t+\Delta t$ by $[K']^{t+\Delta t}\{q\} = {}^{t+\Delta t}\{F'\}$

(vi) Calculate acceleration and velocity at time $t+\Delta t$

$$^{t+\Delta t}\{\ddot{q}\} = a_0\left(^{t+\Delta t}\{q\} - ^{t}\{q\}\right) - a_0\Delta t \times \{\dot{q}\} + \left(1.0 - 2\theta_1^2\right)\{\ddot{q}\} \qquad \textbf{(2. 20)}$$

$$^{t+\Delta t}\{\dot{q}\} = ^{t}\{\dot{q}\} + \Delta t(\theta_1 - 0.5)^{t}\{\ddot{q}\} + (1.5 - \theta_1)\Delta t\, ^{t+\Delta t}\{\ddot{q}\}$$

θ – Method offers an unconditionally stable solution. While determining resultant force from the displacement boundary condition, by solving differential equation for one element, Newmark's method was observed to be giving unstable oscillations in the solution. On the other hand, θ – method was found to be giving stable solution under similar conditions. This is discussed in detail later in Chap 4.

2.2 Methods for Simulation of Dynamic Crack Propagation by FEM

To simulate a crack propagation in solids two different concepts of finite element modelling are in use i.e., stationary mesh procedure and moving mesh procedure. Out of these two, moving mesh procedure, as the name implies involve change of mesh in each step as the crack propagates. This is computationally very intensive. Stationary mesh procedures do not require changes in the mesh in general, and require only change in the boundary and loading conditions. The two procedures are explained in the following Sections.

2.2.1 Stationary Mesh Procedure:

In the simple stationary mesh procedure of modelling linear elastodynamic crack propagation, the nodes ahead of the crack tip are spaced at $V_c\Delta t$ (V_c being crack velocity) and crack propagation is simulated by releasing the node one at a time. However, if a simple node release technique is used, release of constraint on the displacement (at the preceding crack tip) one in one time step induces spurious high frequency oscillations in the finite element solution. To overcome these difficulties, several algorithms have been suggested in the literature to release the node gradually over few time steps.

Keegstra et al.[15,16] suggested a model in which node was not released instantaneously when the force at the crack tip reaches a critical value F_D, which is proportional to dynamic fracture toughness K_D. Instead the force was reduced from F_D gradually in accordance with an elastic spring model so that the nodal force vanish when critical displacement is reached. Another node release technique of gradual release of nodes is 'Force release model'.

2.2.1.1 Force Release Model

Suppose that the actual tip is located at 'C' in between the finite element nodes B and D as shown in Fig 2.1. The length segments BC and BD are b and d respectively. The holding back force ,F, at node B is gradually reduced to zero over a number of time steps as the crack tip reaches to the node D. Various schemes available to decrease the force to zero are as follows:

(i) Malluck and King[17] suggested the release rate based on constant stress intensity factor

$$\frac{F}{F_0}=\left(1-\frac{b}{d}\right)^{\frac{1}{2}} \qquad \textbf{(2. 21)}$$

where F_0 is the original reaction force when the crack tip was located at node B.

(ii) Rydhom et al.[18] Suggested the release rate based on constant energy release rate

$$\frac{F}{F_0}=\left(1-\frac{b}{d}\right)^{\frac{3}{2}} \qquad \textbf{(2. 22)}$$

(iii) Kobayasi et al.[19] suggested the linear release rate based on no physical argument other that pure intuition.

$$\frac{F}{F_0}=\left(1-\frac{b}{d}\right) \qquad \textbf{(2. 23)}$$

In order to have more gradual and smooth propagation of crack Kishore, Kumar and

Verma [20] used a modified method. Holding back force at the crack tip B is linearly decreased to zero when the crack reaches end of the next element. Thus when crack tip goes beyond node B then

$$\frac{F_B}{F_{HB}} = \left(1 - \frac{b}{d + d_1}\right) \tag{2. 24}$$

where F_{HB} is the reaction at node B, when the node was closed, b is the crack extension and d,d_1 are the elements length as shown in Fig 2.1. And when the crack moves beyond node D to a point D_1

$$\frac{F_B}{F_{HB}} = \left(1 - \frac{d + b_2}{d + d_1}\right) \tag{2. 25}$$

$$\frac{F_D}{F_{HD}} = \left(1 - \frac{b_2}{d_1 + d_2}\right) \tag{2. 26}$$

where F_{HD} is the reaction at node D, when the node was closed·

b,b_2 are the crack extension and d,d_1,d_2 are the element lengths as shown in Fig.2.1

In force release model, time increment Δt is usually taken such that it takes 15 to 20 iterations for the crack tip to cross one element. The amount of force necessary to keep the nodes together is determined and a factor is used to proportionately decrease the force as the crack tip advances. Thus, at subsequent times, though the problem is highly dynamic, the current calculations were based on the force calculated to keep the nodes together 15 to 20 time steps before. This will cause discrepancy as the crack advances further from one element to the next one causing large oscillations in the solution. This discrepancy should be overcome for obtaining better solution. A new model is proposed to overcome the drawbacks of force release model which instead of considering dynamic force at the crack tip, takes into account the stiffness and mass of the element at the crack tip. It is described in detail in Chapter 3.

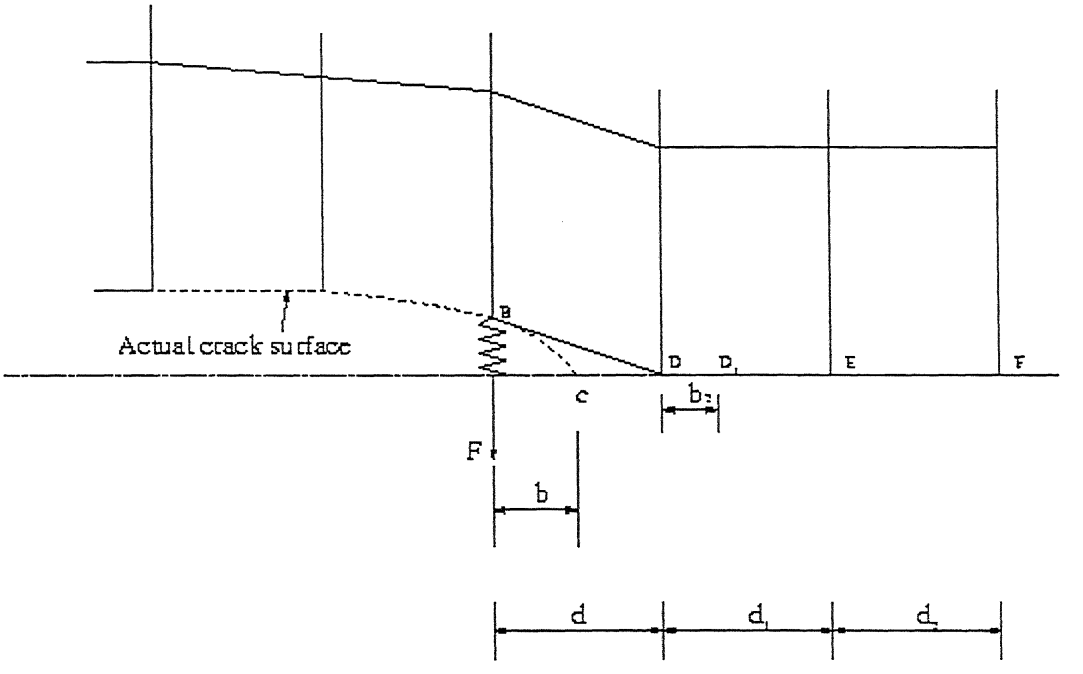

Fig 2.1 Crack opening scheme in force release model

2.2.2 Moving Mesh Procedure:

In moving mesh procedure, entire mesh moves with the crack tip. It can be further classified into an approach wherein a) the entire mesh moves b) only the mesh in a finite and small region around the crack-tip moves along with the crack-tip. Aberson et al. [21,22] used a singular crack-tip element as shown in Fig 2.2(a), which incorporates the first 13 terms of Williams' eigenfunctions[23], appropriate to a stationary crack in a linear elastic body. The crack tip moves within the singular element, between the nodes A and B as shown in Fig 2.2(a). When the crack tip reaches the node B, the mesh pattern is changed suddenly, as illustrated in the figure.

Another attempt at using Williams' eigenfunctions was made by Patterson and Oldale[24,25]. The singular element (Fig 2.2(b)) has 13 nodes and is topologically equivalent to two assembled 8 noded isoparametric elements. The location of the singular element is suddenly changed by a distance equal to the size of the regular element ahead of the crack tip, when the crack tip propagates a critical distance within the singular element. The displacements of the singular element are matched to those of the surrounding solid only at the nodes connected to the regular element. Thus, this model violates the displacement compatibility condition at the interfaces between the singular element and the surrounding regular elements. In another procedure, the singular element translates in each time step for which crack growth occurs. Thus crack tip is always at the centre of the singular element throughout the analysis. The regular elements surrounding the moving singular element are continuously distorted. Mesh pattern around the singular element is periodically readjusted for simulating large amount of crack propagation.

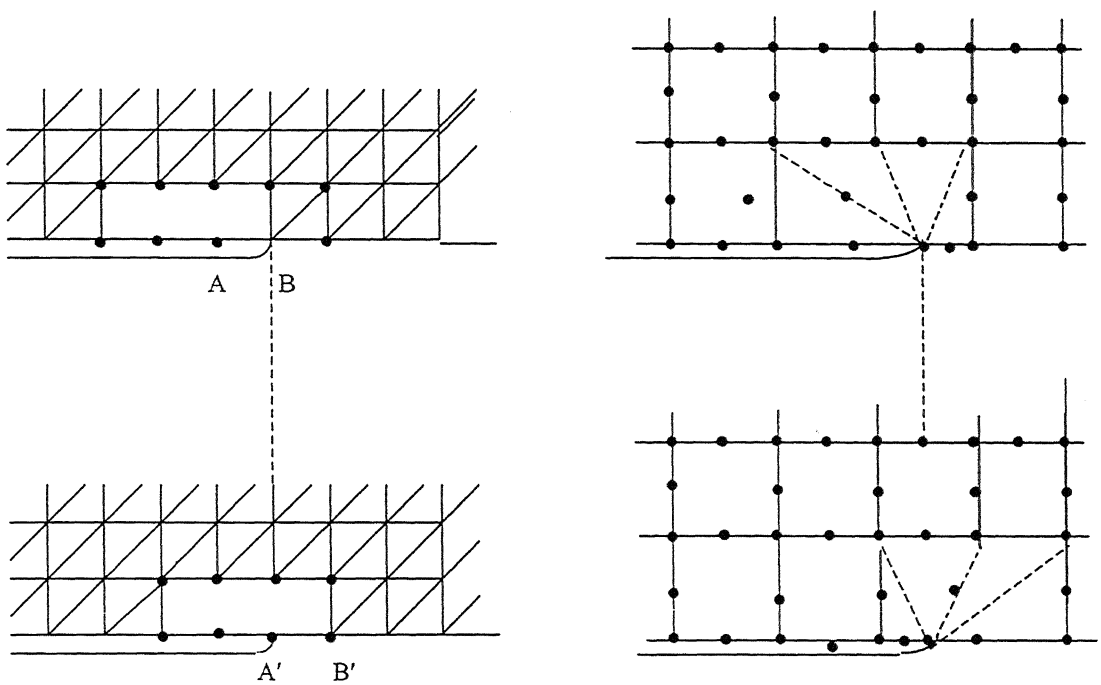

Fig 2.2 Discontinuously moving singular elements

2.3 Energy Release Rate and Its Determination

In fracture mechanics a crack can be characterised by four different parameters

i. Energy release rate (G_I, G_{II}, G_{III}) is energy based and is also applied to brittle and less ductile material
ii. Stress intensity factor (K_I, K_{II}, K_{III}) is stress based. This parameter is also applied to brittle and less ductile material.
iii. J-Integral (J) which has been developed to deal with ductile material and can also be applied to brittle material as well.
iv. Crack tip opening displacement (CTOD) is displacement based and is developed for ductile materials.

From computational point of view, stress intensity factor require special elements so as to simulate stress singularity at the crack tip whereas J-Integral and energy release do not require any such modelling of stress singularity. In energy release rate approach, energy is found out in entire domain and in J-Integral, evaluation is done along a path far away from crack tip. Thus both these approaches adroitly avoid analysis close to the crack tip and don't need any modelling of stress singularity.

Griffith [26] outlined that in brittle fracture, the extension of a crack requires the formation of new surface, he reasoned with its associated surface energy, consequently, crack in a brittle solid should advance when the reduction of the total potential energy of the body during a small amount of crack advance equals the surface energy of the new surface thereby created. Most of the energy release, as the crack advances, comes from the parts of the plate which are adjacent to the cracked surface.

Two important parameters need to be considered

1) How much energy is released when a crack advance
2) Minimum energy required for crack to advance in forming two new surfaces

First parameter is measured in terms of energy release rate denoted by G. G is a function of crack size in general. Energy release rate is the amount of energy release per unit increase in area during crack growth. This energy is supplied by the elastic energy in the body and by the loading system.

The energy requirement for a crack to grow per unit area extension is called as crack resistance and is usually denoted by symbol R. Crack resistance is sum of energy required to 1) form new surface and 2)cause anelastic deformation

Both the available energy release rate and crack resistance are important to study the possibility of crack becoming critical. Obviously, when the available energy release rate far exceeds the crack resistance, the crack starts to grow at high speed.

In the present study 'energy release rate' is adopted as it is a more comprehensive concept.

As the crack advances,

1) Stiffness of the component decreases.
2) Strain energy in the component either increases or decreases.
3) Work is done on the component if there is an application of load.
4) Energy is being consumed to create two new surfaces.

For quasi-static growth of crack by crack area ΔA, the incremental work by external force be ΔW_{ext}, change in strain energy be ΔU, and the available energy, GΔA, satisfy energy balance equation.

$$G\Delta A = \Delta W_{ext} - \Delta U \tag{2. 27}$$

$$G = -\frac{d}{dA}(U - W_{ext}) \tag{2. 28}$$

$$G = -\frac{d\Pi}{dA} \tag{2. 29}$$

where Π is the potential energy

For a plate of uniform thickness, dA=Bda

where da is the incremental crack length

B is the thickness of the plate

$$G = -\frac{1}{B}\frac{d\Pi}{da} \tag{2. 30}$$

For dynamic crack propagation problem, the kinetic energy ,T, of the body should be taken into consideration. Dynamic energy release rate , G_D, is different as some energy may be consumed to impart kinetic energy to the cracked portion of the body and to generate stress waves.

For dynamic case, energy balance becomes

$$G\Delta A = \Delta W_{ext} - \Delta U - \Delta T \tag{2. 31}$$

where ΔT is the increment in kinetic energy in the body.

For constant velocity crack propagation,

$$G = \frac{1}{B}\frac{d}{da}(W_{ext} - U - T) \tag{2. 32}$$

For crack moving with velocity v,

$$G = \frac{1}{B}\frac{\frac{d}{dt}(W_{ext} - U - T)}{v} \tag{2. 33}$$

In the present study, Energy release rate is found out using equation (2.17). Different energies are found out using

$$W_{ext} = \{Q\}^T\{F\} \tag{2. 34}$$

$$[U] = \frac{1}{2}\{Q\}^T[K]\{Q\} \tag{2. 35}$$

$$T = \frac{1}{2}\{\dot{Q}\}^T[M]\{\dot{Q}\} \tag{2. 36}$$

where

W_{ext} is the external work done

U is the strain energy in the component

T is the kinetic energy in the component

$\{F\}$ is the external force vector

$\{q\}$ is the displacement vector

$\{\dot{q}\}$ is the velocity vector

$[K]$ is global stiffness matrix

$[M]$ is global mass matrix

2.4 Closure

In this Chapter, formulation of FEM equation is described along with integration algorithms for solving equilibrium equation governing linear dynamic response of a system of finite element. Various methods of simulating dynamic crack propagation with stationary mesh and moving mesh are described. This Chapter also describes some general concepts in energy and energy release rate which will be used in the next Chapters to construct a propagation element.

CHAPTER 3

CRACK PROPGATION ELEMENT

3.1 Introduction

Existing force release models have certain shortcomings, such as,

1. They give rise to very high oscillations in the solution.
2. They are not suitable for solving inverse problem in crack propagation. If the crack propagates and stops in between an element and starts again later when another stress wave arrive, how much holding force to be used is not known.

In the following sections, a propagation model with modified stiffness and mass matrices are presented to take into account of the crack extension.

3.2 Stiffness Release Model

In stiffness release model[12], one-dimensional elastic element is added at the crack tip node, whose stiffness is reduced gradually as crack tip advances to the next node (Fig 3.1). Additional stiffness required is very large when crack tip is at the beginning of element and zero when crack tip reaches to the other end. Amount of additional stiffness required is a function of crack length and is obtained from quasi-static crack propagation analysis.

Fig 3.1(a) shows a symmetric part of deformed 2-D plate in which crack is at node B, gradually propagating to an intermediate position in between node B and node C

Fig 3.1(b), modeled by addition of spring element and finally crack reaching node C Fig 3.1(c).

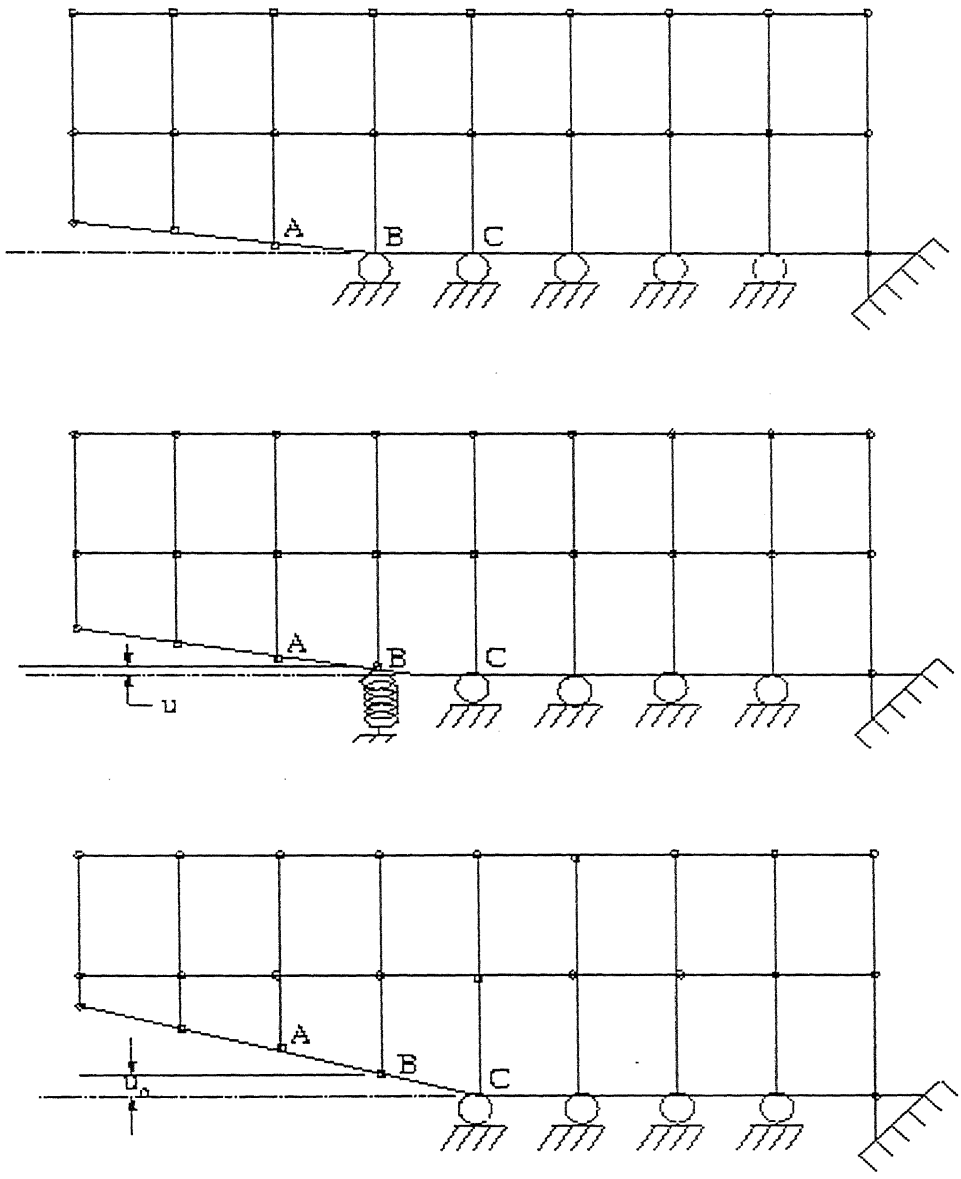

Fig 3.1 Crack opening pattern in model

Let,

K_0 be the stiffness at node B of original plate without additional spring

u_0 be the displacement of node when crack tip reaches the next node and element opens up completely.

K_s can be found out from equilibrium equation as

$$\mathbf{K}_0(\mathbf{u}_0 - \mathbf{u}) = \mathbf{K}_s\mathbf{u} \tag{3.1}$$

$$K_s = K_0\left[\frac{u_0}{u} - 1\right] \tag{3.2}$$

Energy in the spring is given as

$$E_s = \frac{1}{2}K_s u^2 = \frac{1}{2}K_0\left[\frac{u_0}{u} - 1\right]u^2 \tag{3.3}$$

Energy release rate is written as

$$G = \frac{\Delta E}{\Delta A} \tag{3.4}$$

where ΔA is the increment in crack area

Let a non-dimensional parameter for crack length (a) be defined as,

a=crack length (within element) / d

where d is the distance between two nodes.

$\therefore \Delta A = Bd\Delta a$

where B is the thickness of plate.

For static case, energy release rate for a double cantilever beam can be written as

$$G = \frac{1}{2}K_0(-u_0)\frac{1}{Bd}\frac{du}{da} \tag{3.5}$$

Assuming linear variation of G and a, G can be written as

$$G = C_1 + C_2 a \tag{3.6}$$

where, C_1 and C_2 are the constants to be determined.

Substituting G in equation (3.5)

$$C_1 + C_2 a = -\frac{1}{2}\frac{K_0 u_0}{Bd}\left(\frac{du}{da}\right) \tag{3.7}$$

On integrating equation (3.7)

$$u = -\frac{2}{K_0 u_0} Bd\left(C_1 a + \frac{C_2 a^2}{2} + C_0\right) \tag{3.8}$$

On substituting

initial condition u=0 when a=0

end condition $u=u_0$ when a=1

$$u_0 = -\frac{2}{k_0 u_0} Bd\left(C_1 + \frac{C_2}{2}\right) \tag{3.9}$$

Eq.(3.8) and Eq.(3.9) gives

$$\frac{u}{u_0} = \frac{2C_1 a + C_2 a^2}{2C_1 + C_2} \tag{3.10}$$

On simplification it reduces to

$$\frac{u}{u_0} = a + C(a - a^2) = f \qquad (3.11)$$

where

$$C = -\left(\frac{C_2}{2C_1 + C_2}\right) \qquad (3.12)$$

Eq. (3.2) finally can be written as

$$K_s = K_0\left(\frac{1-f}{f}\right) \qquad (3.13)$$

where $f=u/u_0$ as given by Eq (3.11)

Static stiffness K_0 can be determined for a given specimen under static condition. Energy release rate is determined using Eqn (3.5) and (3.11).

However as Eqn 3.5 was based on quasi-static crack propagation, it doesn't take into account the kinetic energy in the body. In dynamic problem total energy comprise strain energy in the body, kinetic energy and work done by external forces. For finding energy release rate, drop in the total energy in the system is considered in the present model and energy release rate is determined using fundamental Eqn (2.15)

Effect of Constant 'C'

Constant 'C' in equation (3.11) can be determined for quasi-static case so as to get a straight-line variation of energy release rate curve. For quasi-static case this value is very small. However it was observed that C has considerable effect in dynamic crack propagation. Effect of change in value of C on f Vs a curve is shown in fig (3.2)

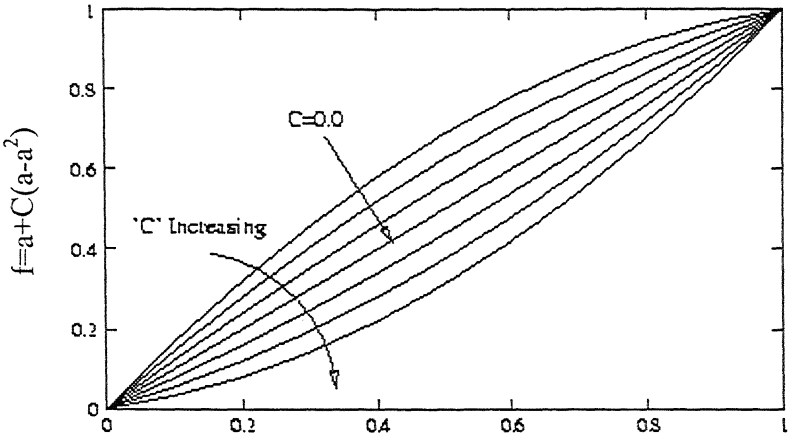

Fig. 3.2 f Vs a curve for different C

Spring stiffness ,K_s, which is gradually reduced as the crack propagates, is a function of crack length 'a' and constant C. This constant, C, is affected by change in element size and time step Δt. For a given problem, its value need to be chosen so that final energy release rate curve are smooth without wide fluctuation.

Although the proposed stiffness K_s of the additional elastic spring element varies from ∞ to 0, it changes discretely in a finite number of steps as the crack propagates through one element. For example, if the number steps to cross one element is considered as 10, then 'a' varies from 0.1 to 1.0 in steps of 0.1. Instead of finding K_s at discrete points, an approach of averaging values over each step is adopted. This is brought about by averaging 'f ' in Eq.3.11 in between for each small step and then finding out K_s using Eq. 3.13. It is observed that averaging the values of f in each step gives smoother variation of energy release rate. This effect will be illustrated later in Chapter 4.

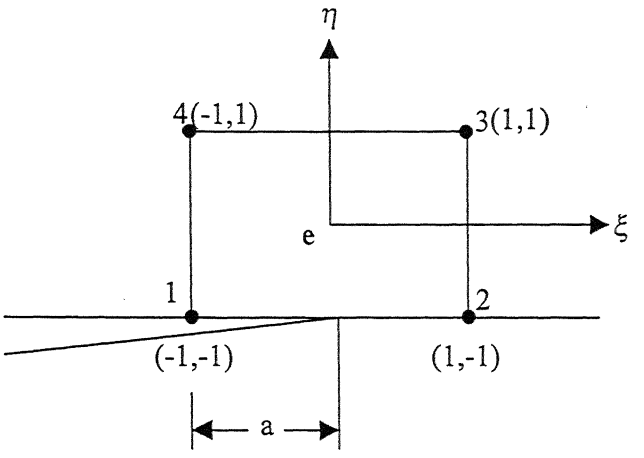

Fig 3.3 Representation of an element at the crack tip

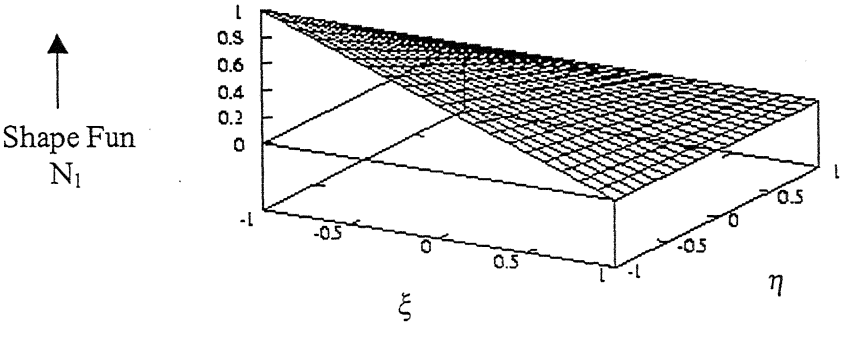

Fig 3.4 Shape fun N_1 for a=1.0

In order to bring the effect of mass variation, shape function N_1 of the element at the crack tip is modified in such a way that it is a function of non dimensional crack length 'a' .

In the present work modified N_1 is proposed as,

$$N_1 = \left(\frac{1-\xi}{2}\right)^{\alpha}\left(\frac{1-\eta}{2}\right) \qquad \textbf{(3. 18)}$$

where

$$\alpha = \left(\frac{10(1.1-a)}{a}\right)^{0.9} \qquad \textbf{(3. 19)}$$

N_1=1 when $\xi = \eta = -1$

=0 when $\xi = \eta = 1$

α is chosen such that, for a given crack length (a) within an element

N_1=1 when ξ= -1

=0 when $\xi \geq (2a-1)$

for example with a=0.5,

N_1=1 for ξ= -1

=0 for $\xi \geq 1$ or $a \geq 0.5$

Thus as the crack advances, shape function N_1 varies in such a way that mass of the element increases gradually. Finally when a=1 i.e., when crack is at the end of the element, shape function N_1 take its bilinear form. Variation of N_1 along crack axis for various crack lengths is as shown in fig (3.5) and the surface plot of N_1 for a=0.5 is shown in fig (3.6).

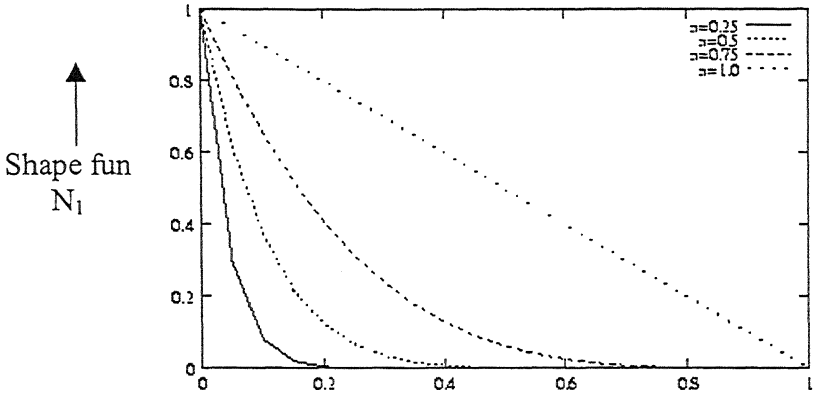

Fig 3.5 Variation of shape function N_1 Vs crack length a (η= -1)

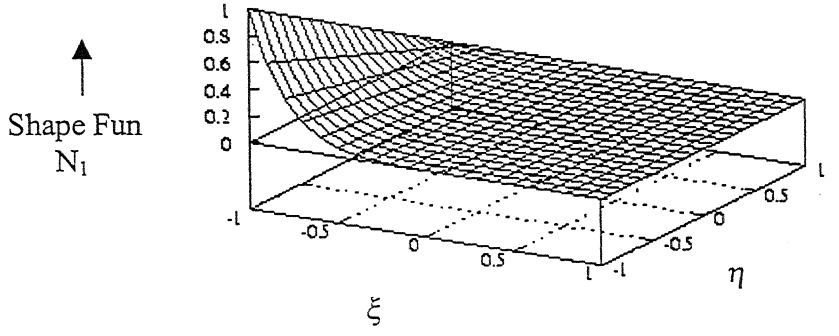

Fig 3.6 Shape fun N_1 for a=0.5

With modified shape function, element mass matrix given by Eqn (2.8) get modified. The effected coefficients are:

$$M_{11} = M_{22} = \int_{\Omega^{(e)}} \left(\frac{1-\xi}{2}\right)^{2\alpha} \left(\frac{1-\eta}{2}\right)^{2} |J| d\xi d\eta \qquad \textbf{(3. 20)}$$

$$M_{12} = M_{21} = 0 \qquad \textbf{(3. 21)}$$

$$M_{13} = M_{31} = M_{24} = M_{42} = \int_{\Omega^{(e)}} \left(\frac{1-\xi}{2}\right)^{\alpha} \left(\frac{1-\eta}{2}\right)^{2} \left(\frac{1-\eta}{2}\right)^{2} |J| d\xi d\eta \qquad \textbf{(3. 22)}$$

$$M_{14} = M_{41} = M_{23} = M_{32} = 0 \qquad \textbf{(3. 23)}$$

$$M_{15} = M_{51} = M_{26} = M_{62} = \int_{\Omega^{(e)}} \left(\frac{1-\xi}{2}\right)^{\alpha} \left(\frac{1+\xi}{2}\right) \left(\frac{1-\eta^{2}}{4}\right) |J| d\xi d\eta \qquad \textbf{(3. 24)}$$

$$M_{16} = M_{61} = M_{25} = M_{52} = 0 \qquad \textbf{(3. 25)}$$

$$M_{17} = M_{71} = M_{28} = M_{82} = \int_{\Omega^{(e)}} \left(\frac{1-\xi}{2}\right)^{\alpha+1} \left(\frac{1-\eta^{2}}{4}\right) |J| d\xi d\eta \qquad \textbf{(3. 26)}$$

$$M_{18} = M_{81} = M_{27} = M_{72} = 0 \qquad \textbf{(3. 27)}$$

Comparative figures of elemental mass matrices for a=0.5 and a=1.0 are shown Fig 3.7 (a) and (b) respectively.

For a=1.0

$$[M]^{(e)} = \begin{bmatrix} 10.45 & 0.00 & 5.23 & 0.00 & 2.61 & 0.00 & 5.23 & 0.00 \\ 0.00 & 10.45 & 0.00 & 5.23 & 0.00 & 2.61 & 0.00 & 5.23 \\ 5.23 & 0.00 & 10.45 & 0.00 & 5.23 & 0.00 & 2.61 & 0.00 \\ 0.00 & 5.23 & 0.00 & 10.45 & 0.00 & 5.23 & 0.00 & 2.61 \\ 2.61 & 0.00 & 5.23 & 0.00 & 10.45 & 0.00 & 5.23 & 0.00 \\ 0.00 & 2.61 & 0.00 & 5.23 & 0.00 & 10.45 & 0.00 & 5.23 \\ 5.23 & 0.00 & 2.61 & 0.00 & 5.23 & 0.00 & 10.45 & 0.00 \\ 0.00 & 5.23 & 0.00 & 2.61 & 0.00 & 5.23 & 0.00 & 10.45 \end{bmatrix} \times 10^{-6}$$

(a)

For a=0.5

$$[M]^{(e)} = \begin{bmatrix} 0.93 & 0.00 & 0.33 & 0.00 & 0.17 & 0.00 & 1.27 & 0.00 \\ 0.00 & 0.93 & 0.00 & 0.33 & 0.00 & 0.17 & 0.00 & 1.27 \\ 0.33 & 0.00 & 10.45 & 0.00 & 5.23 & 0.00 & 2.61 & 0.00 \\ 0.00 & 0.33 & 0.00 & 10.45 & 0.00 & 5.23 & 0.00 & 2.61 \\ 0.17 & 0.00 & 5.23 & 0.00 & 10.45 & 0.00 & 5.23 & 0.00 \\ 0.00 & 0.17 & 0.00 & 5.23 & 0.00 & 10.45 & 0.00 & 5.23 \\ 1.27 & 0.00 & 2.61 & 0.00 & 5.23 & 0.00 & 10.45 & 0.00 \\ 0.00 & 1.27 & 0.00 & 2.61 & 0.00 & 5.23 & 0.00 & 10.45 \end{bmatrix} \times 10^{-6}$$

(b)

Fig 3.8 **Elemental mass matrix for a=1.0 and a=0.5**

By modifying shape function of elemental mass matrix, mass of the element is made to vary as a function of crack length. Element mass is zero when the crack is at the beginning of the node and increases gradually till crack reaches to the end of the element, when mass of the element becomes equal to the mass of a regular element. Effect of this modification on energy release rate variation will be shown in Chap 4.

3.4 Closure

Chapter 3 described in details of variation of various aspects of the proposed model. This model will be investigated with hypothetical data as well as experimental data in Chap 4. Effect of various parameters on energy release rate will be described in the succeeding chapter.

CHAPTER 4

RESULTS AND DISCUSSION

4.1 Introduction

In this Chapter results of the dynamic crack propagation analysis are presented using the method described in the previous Chapters. First the method is validated for both quasi-static case and dynamic case. Later results are also presented for the available experimental data for crack propagation.

Various aspects of the results involve,

- Determination of C for quasi-static crack propagation.
- Crack propagation at constant speed under dynamic input force pulse
- Crack propagation at constant speed under time dependent input displacement (based on experimental data)

4.2 Validation of the Proposed Model

For the analysis purpose of investigating various aspects, a hypothetical problem of cantilever beam specimen is considered (Fig 4.1(a)). Due to symmetry only upper half portion is taken into account(Fig 4.1(b)).

Material and geometric properties are as follows

- Modulus of Elasticity $E=210x10^9$ N/m^2
- Poisson ratio $\nu=0.3$
- Length of specimen $L=0.06$m

- Width of specimen W=0.005m
- Thickness of specimen B=0.024m
- Crack length a′=0.03m

The problem is symmetric and only one half is considered for descritisation and analysis. The DCB specimen is analysed by using 4-noded isoparametric element. Details are as follows

- Number of elements 600
- Number of nodes 671
- Size of element in X-dir 1.0mm
- Size of element in Y-dir 0.5mm

For dynamic crack propagation, a short pulse is applied at the top of the specimen(Fig 4.2). The pulse can be modelled by F(1-cos(ωt)) whose details are as follows:

- Pulse duration p=8μs
- Force amplitude F_0=50N
- Frequency of pulse f′=125KHz

Time step Δt depends on the element size and wave velocity.

4.3 Determination of C from Quasi-Static Case

For quasi-static case, mass of matrix is essentially zero and it is only additional stiffness of elastic element, which will vary from maximum (infinity) to zero. Static stiffness K_0 can be determined for a given mesh by applying force at the node preceding crack tip node and measuring corresponding displacement at that node.

For quasi-static case, a wedge loaded DCB specimen is considered with a constant displacement equal to 0.025×10^{-3}m at the crack opening. Energy release rate variation due to crack propagation is as shown in Fig 4.3 Curves are plotted for different values of constant C. It is observed that, for C= -0.01 and C=0.0 though G is continuous within the element, it is not continuous from element to element. On the other hand for C= -0.028, G curve is continuous both within the element and also across element boundaries.

These C values may not be suitable for dynamic case. However, this forms the initial guess value.

4.4 Dynamic Crack Propagation

For dynamic crack propagation study, the same DCB specimen data as mentioned in Sec 4.2 is considered. Crack propagation starts after the force pulse of 8μs is completely applied.

For all the cases following parameters are taken

i. Crack initiation time 8μs

ii. Crack speed 1500m/s

Two different time steps are considered.

Before crack propagation $\Delta t_1 = 1.0 \times 10^{-6}$sec

After crack propagation initiates Δt_2 a reduced value for higher accuracy

4.4.1 Effect of Change in Value of C

As obtained earlier in Sec 4.3 for quasi-static case, value of constant C for straight-line variation of energy release rate is C= -0.028. The same value when used for dynamic case gives energy release rate variation for crack velocity equal to 1500m/s as shown in Fig 4.4

Thus it can be seen from Fig 4.4 that there are large oscillations at the inter element boundaries. Besides this there are smaller oscillations within the element. It clearly shows that C value for the quasi-static case is not suitable for the dynamic case and has to be modified. Variation of C values causes effective stiffness value at the crack tip (in vertical direction), to vary as shown in Fig 4.5. C value is adjusted so that the energy release rate curve becomes smoother. Effect of change in C value on energy release rate curve is shown in Fig 4.6. It can be seen that C=0.4 gives rise to less oscillations in G_I in comparison to other values and it is chosen for further analysis.

4.4.2 Dynamic Crack Propagation with Averaging of 'f'

As illustrated in Sec 3.7.2 since only finite number of steps are considered for the crack propagation in one element. The zone between zero and first step goes unconsidered. So a method of averaging the values of 'f' in Eqn. 3.11 is considered.
Fig 4.7 shows difference in energy release rate curve for the same value of constant C.
Figure clearly shows that energy release rate curve with averaged value of 'f ' gives better solution.

4.4.3 Effect of Shape Function modification on Element Mass Matrix

As the stiffness of elastic element decreases gradually to zero, the element mass can be increased from 0 to its usual value by modifying shape function N_1 for element mass matrix for an element containing propagating crack (Sec 3.5). Energy release rate after this modification is as shown in Fig 4.8. Fig reveals that final energy release rate curve gives smooth variation within element and fairly stable solution across element boundaries.
Similar results for crack velocity of 1250m/s are shown in Fig 4.9. It can be seen very clearly that solution with mass modification is better than one without mass modification.

4.4.4 Effect of element size and time step

In the present model, for simulating dynamic crack propagation, both stiffness as well as mass matrix are modified for the element containing crack tip. For the crack tip node the effective combined stiffness and mass matrix value in the time integration scheme (Newmark's method) is

$$K' = K + \frac{1-f}{f} K_0 + a_0 \hat{M} \tag{4.1}$$

$$= K + K_s + a_0 M \tag{4.2}$$

where,

K_s is stiffness of elastic element and

a_0 is a Newmark's integration constant

$$a_0 = \frac{1}{\alpha \Delta t^2} \tag{4.3}$$

Thus effective stiffness K′ depends on, K which in turn depends on size of element, K_s which is a function of crack length and static stiffness value K_0. And a_0 depends on time step Δt, $\hat{M}$ which is a function of crack length 'a'. Fig (4.10) shows the nature of $(K + K_s)$ Vs non-dimensional crack length. $(K + K_s)$ is a monotonically decreasing curve and is independent of change in time step, Δt. Fig (4.11) show variation of $a_0 M$ with 'a'. This curve has increasing variation with crack length. One important point to be recognised is that decrease in Δt by half increases $a_0 M$ four folds. Fig 4.12 shows the combination of all terms giving by Eqn(4.2) and represents effective stiffness matrix at the crack tip node.

Following observation can be made

1. For $\Delta t = 0.13 \mu s$ effective stiffness matrix has a monotonically decreasing nature

2. For $\Delta t = 0.067\mu s$, the curve decreases and then increases in the later half of the but otherwise it's a smoothly decreasing curve.
3. For $\Delta t = 0.033\mu s$ inertial term becomes dominant and effective stiffness is no longer a continuously decreasing curve. There is large sag in the middle of the curve.

Fig 4.13 reveals its effect on energy release rate curve.

1. For $\Delta t = 0.13\mu s$ because of higher time step inertial term has a negligible contribution and energy release rate has variation close to the case without mass modification case.
2. For $\Delta t = 0.067\mu s$ there is a balanced contribution from mass and stiffness. Energy release rate curve gives smooth variation throughout crack length.
3. For $\Delta t = 0.033\mu s$ oscillations are appearing both within the element as well as across inter element boundaries.

These leads to conclusion that size of the element and time step (Δt) should be chosen in such that K′ decrease fairly monotonically.

4.5 Crack Propagation in Glass Fabric/Epoxy DCB Specimen

The present method is applied to determine the dynamic G_I for the experimental data as reported by Chowdhary[27] .

From the mechanics point of view fibre composites are among the class of material called orthotropic materials. Generalised Hook's Law for 2-D orthotropic laminate is given by Agarwal[28].

$$\sigma_{ij} = Q_{ij}\varepsilon_{ij} \qquad (4.4)$$

i,j=1,2….,6

where σ_i are the stress components, Q_{ij} is the stiffness matrix, ε_j are engineering strain components.

For 2-D orthotropic material,

$$\begin{Bmatrix} \sigma_1 \\ \sigma_2 \\ \tau_{12} \end{Bmatrix} = \begin{bmatrix} Q_{11} & Q_{12} & 0 \\ Q_{21} & Q_{22} & 0 \\ 0 & 0 & Q_{66} \end{bmatrix} \begin{Bmatrix} \varepsilon_1 \\ \varepsilon_2 \\ \gamma_{12} \end{Bmatrix} \tag{4.5}$$

where,

$$Q_{11} = \frac{E_L}{1 - \upsilon_{LT}\upsilon_{TL}} \tag{4.6}$$

$$Q_{22} = \frac{E_T}{1 - \upsilon_{LT}\upsilon_{TL}} \tag{4.7}$$

$$Q_{12} = \frac{\upsilon_{TL}E_L}{1 - \upsilon_{LT}\upsilon_{TL}} = \frac{\upsilon_{LT}E_T}{1 - \upsilon_{LT}\upsilon_{TL}} \tag{4.8}$$

$$Q_{66} = G_{LT} \tag{4.9}$$

E_L and E_T are elastic modulae in Longitudinal and Transverse direction
G_{LT} is the shear modulus associated with axes of symmetry
υ_{LT} and υ_{TL} are major and minor Poisson ratios.

Relation between four of the five elastic constants is

$$\frac{E_L}{E_T} = \frac{\upsilon_{LT}}{\upsilon_{TL}} \tag{4.10}$$

Following data is used as input for finding energy release rate.

- Displacement at cantilever end as a function of time
- Velocity of crack propagation
- Material data and specimen geometry

Material and geometric properties are as follows

- Material type — Glass fabric/epoxy laminate
- Material density — $\rho=1825 Kg/m^3$
- Elasticity constants — $E_L=26x10^9 N/m^2$
  $E_T=6.6x10^9 N/m^2$
  $G_{LT}=3.5x10^9 N/m^2$
- Poisson ratio — $\nu_{LT}=0.21$
  $\nu_{TL}=0.05331$

3 different experimental data is used.

Details of geometric data is given in Table 4.1

Table 4.1 Details of specimen

Expt No	L(mm)	W(mm)	B(mm)	a' (mm)
1	7.8	4.0	24.7	40.4
2	7.6	3.8	25.1	40.3
3	7.6	3.8	24.8	40.0

L – Length of the DCB specimen

W – Width of specimen

B – Thickness of specimen

a' - Crack length

In the experiment, time history of displacement at the cantilever end is known. Fig 4.14, Fig 4.15 and Fig 4.16 gives displacement applied at the cantilever end as a function of time. For determining work done, it is essential to obtain equivalent force as a function of time applied at the cantilever end. Nodal force is obtained from finite element equation.

Resultant of equilibrium force obtained for a typical case is shown in Fig 4.17. It is evident that there are very high oscillations in the solution due to instability of the integration algorithm.

A more stable scheme for solving differential equation the Theta method summarised in Sec 2.13 is used. The difference in the results by these two schemes are shown in Figs 4.17 and 4.18. Thus, oscillations in the equivalent force have reduced drastically. Small oscillations that are still left are finally eliminated by using smooth Bezier curve, which gives equivalent load curve as shown in Fig 4.19.

Fig 4.20-4.22 give the dynamic G_I for these experimental data and results are summarised in Table 4.2

Table 4.2 Initiation and propagation toughness with 'Force release model' and 'present' model:

Expt No	V (m/s)	T_{ini} (s)	G_{ini} (J/m^2)		Gprop (J/m^2)	
			FRM[27]	Present	FRM[27]	Present
1	1233	54.04	418	270	11	4.5
2	1367	45.97	116	52	9	3.4
3	860	44.86	52	19	18	5

Energy release rate variation for experiment no 1,2 and 3 are shown in Fig 4.20, Fig 4.21 and Fig 4.22 respectively. Similar results for force release model is shown in Fig 4.23, Fig 4.24 and Fig 4.25

It is worth noting that energy release rate curve obtained by present analysis is much smoother and can be used for finding propagation toughness.

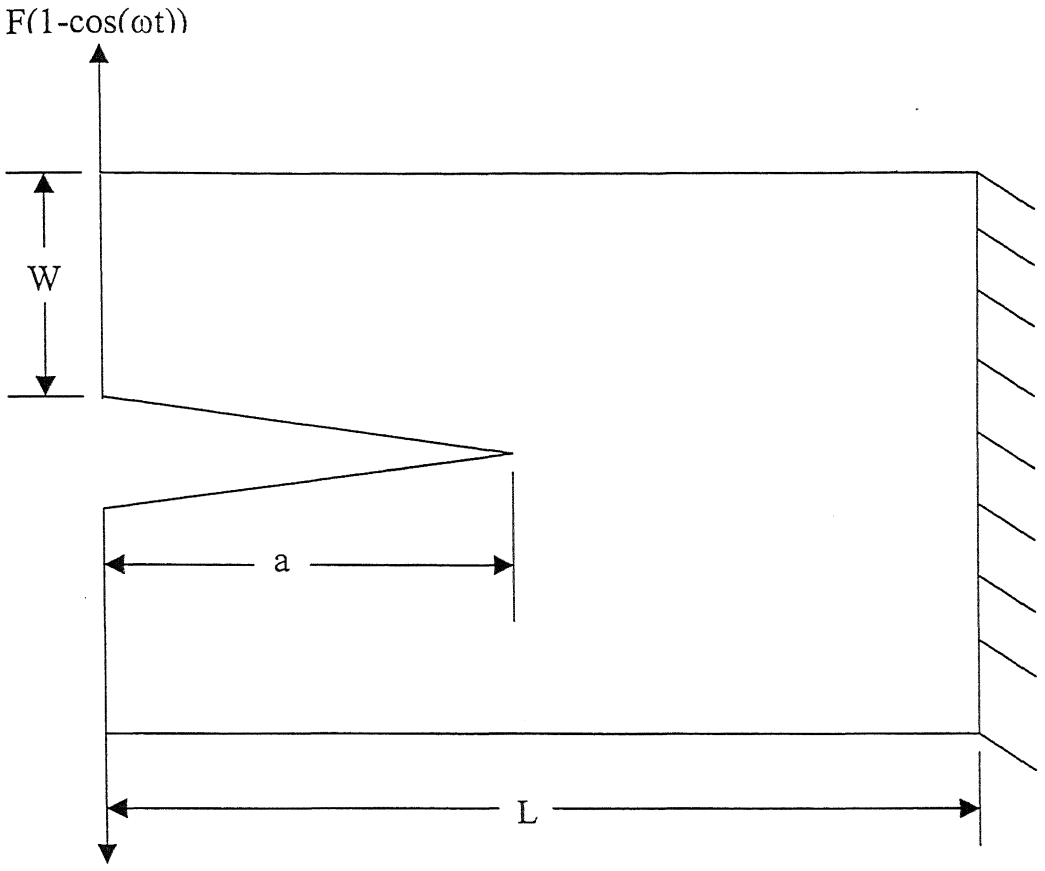

Fig 4.1 DCB Specimen (Full)

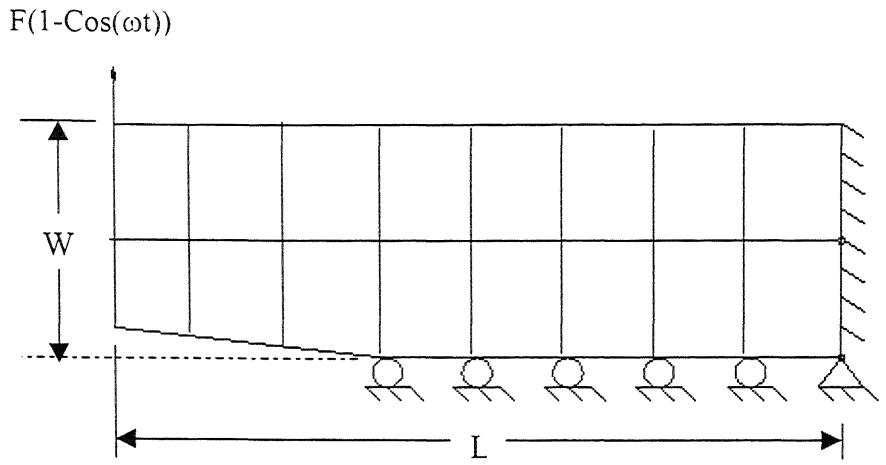

Fig 4.1(b) DCB specimen (Half)

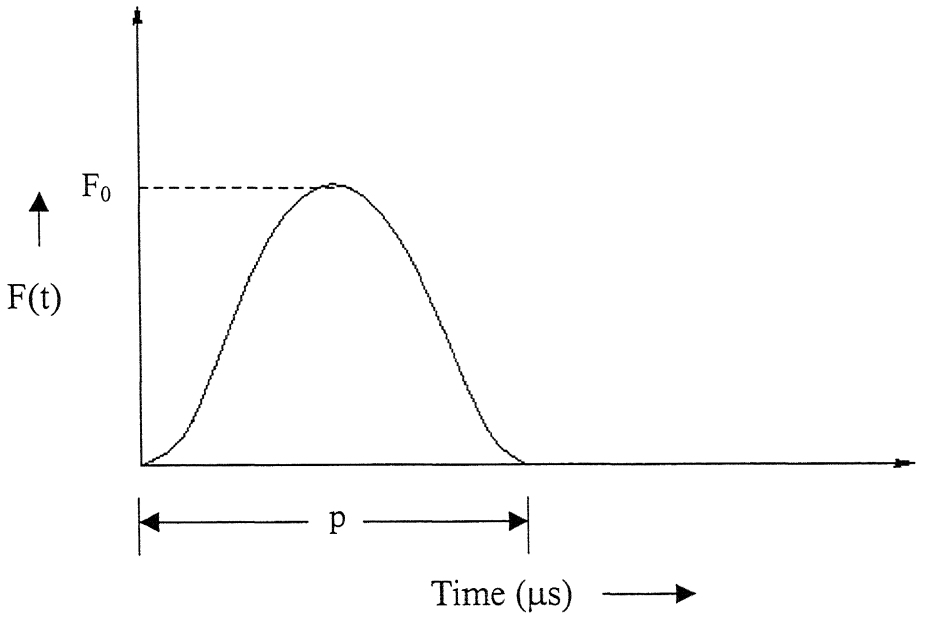

Fig (4.2) Input Force Pulse

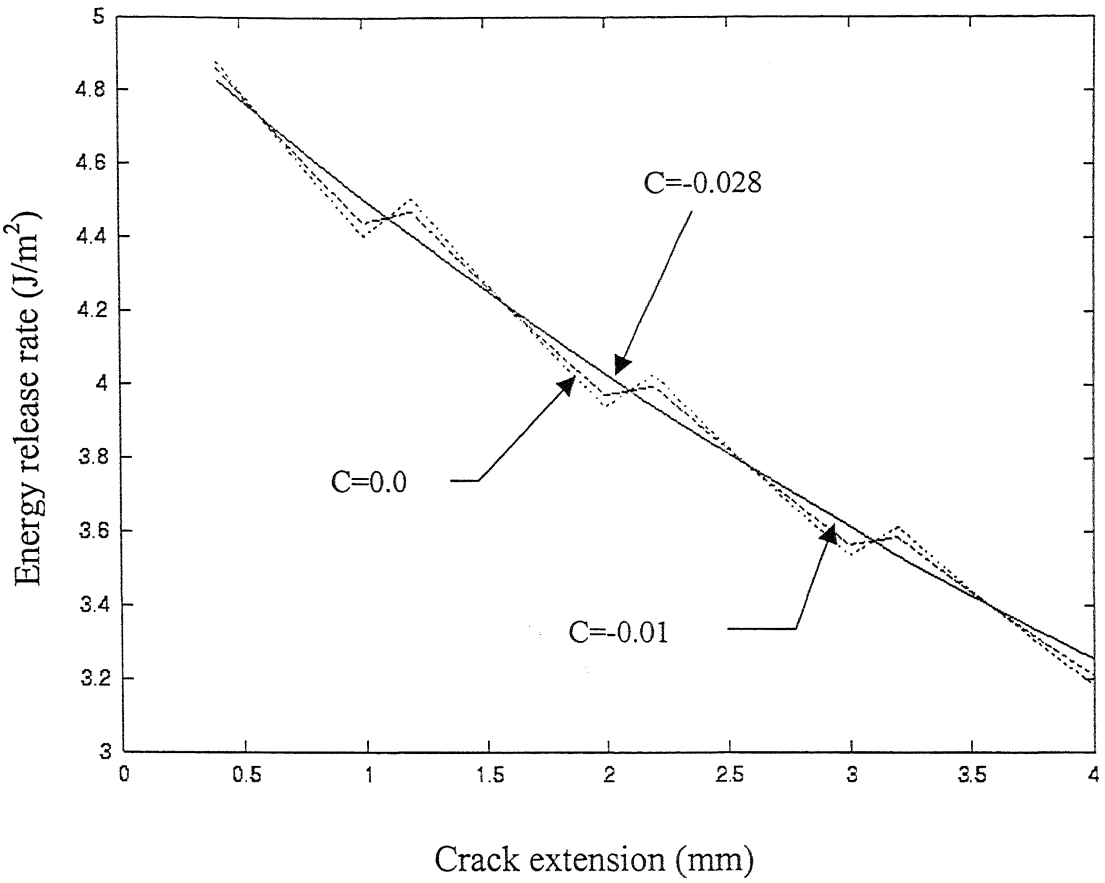

Fig 4.3 Energy release rate variation for quasi-static crack propagation

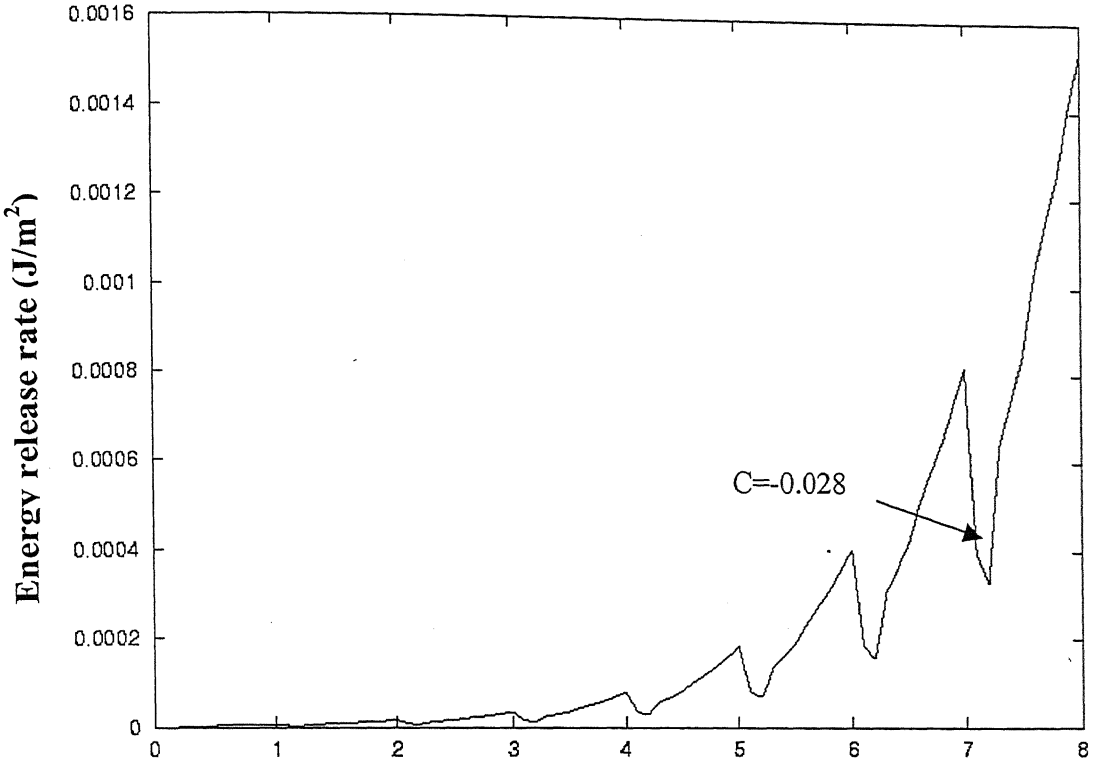

Fig 4.4 Energy release rate variation for crack velocity 1500m/s and q-s C value

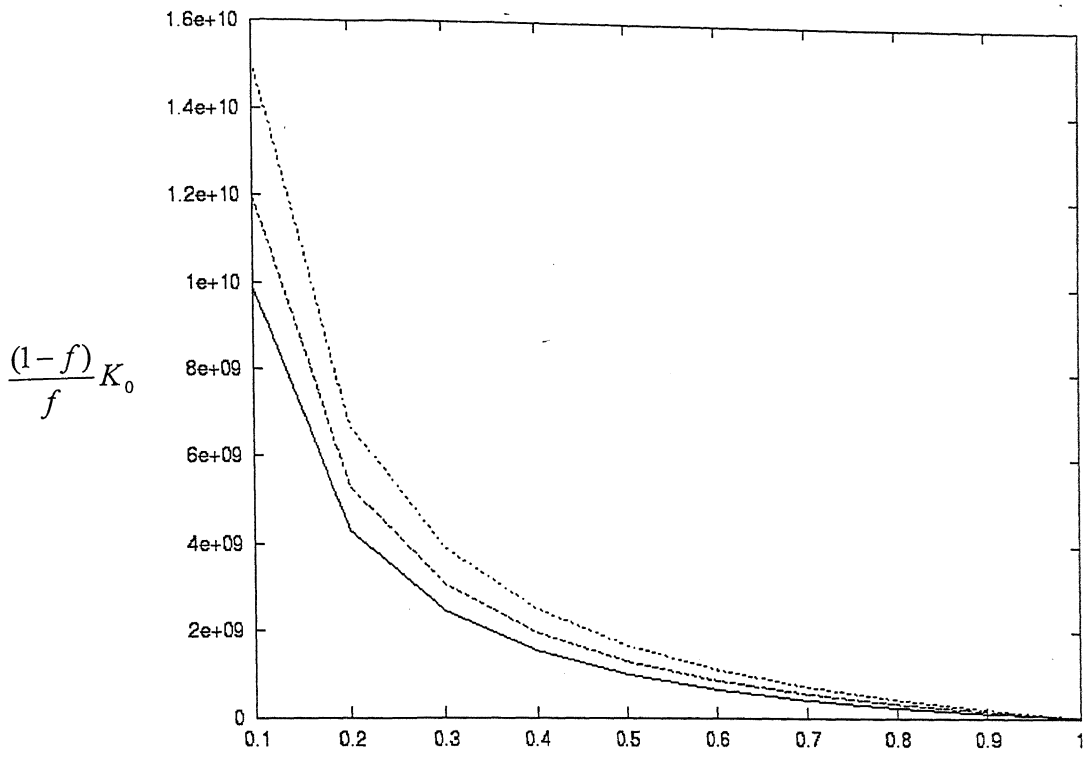

Fig 4.5 Effect of change in C on effective stiffness value at the crack tip

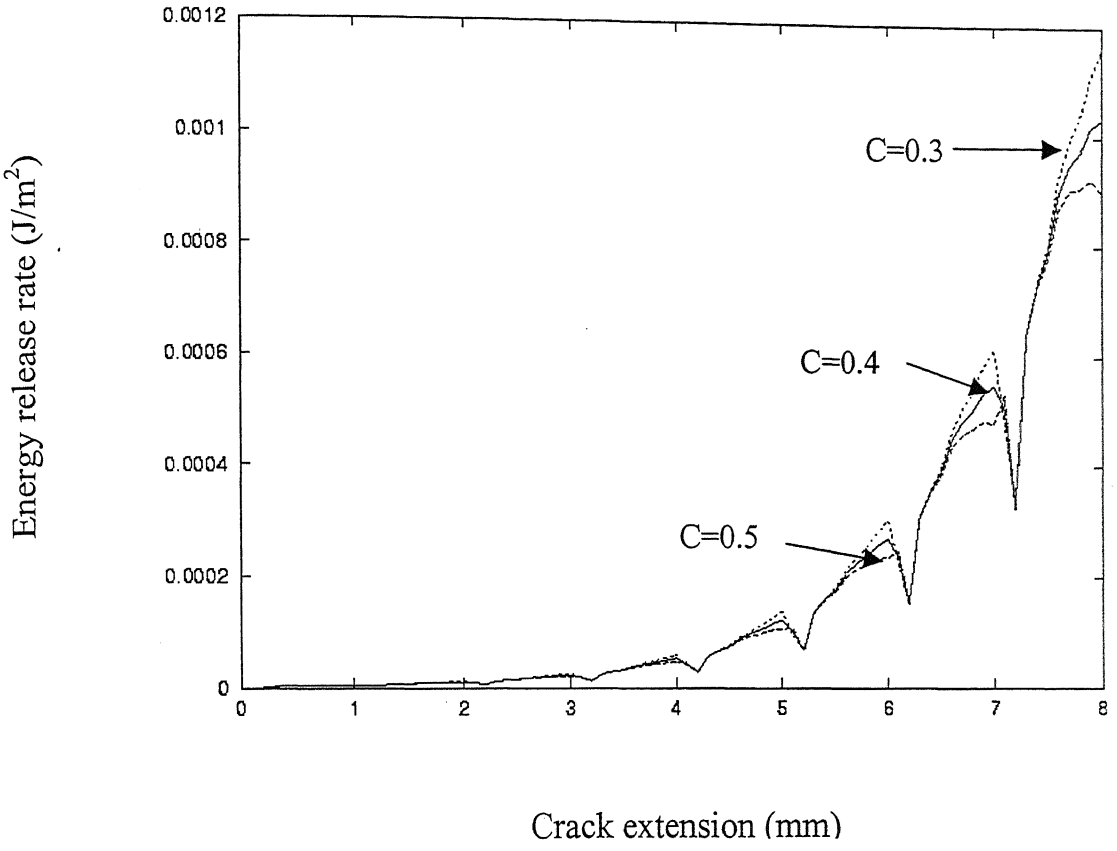

Fig 4.6 Effect of change in C on energy release rate

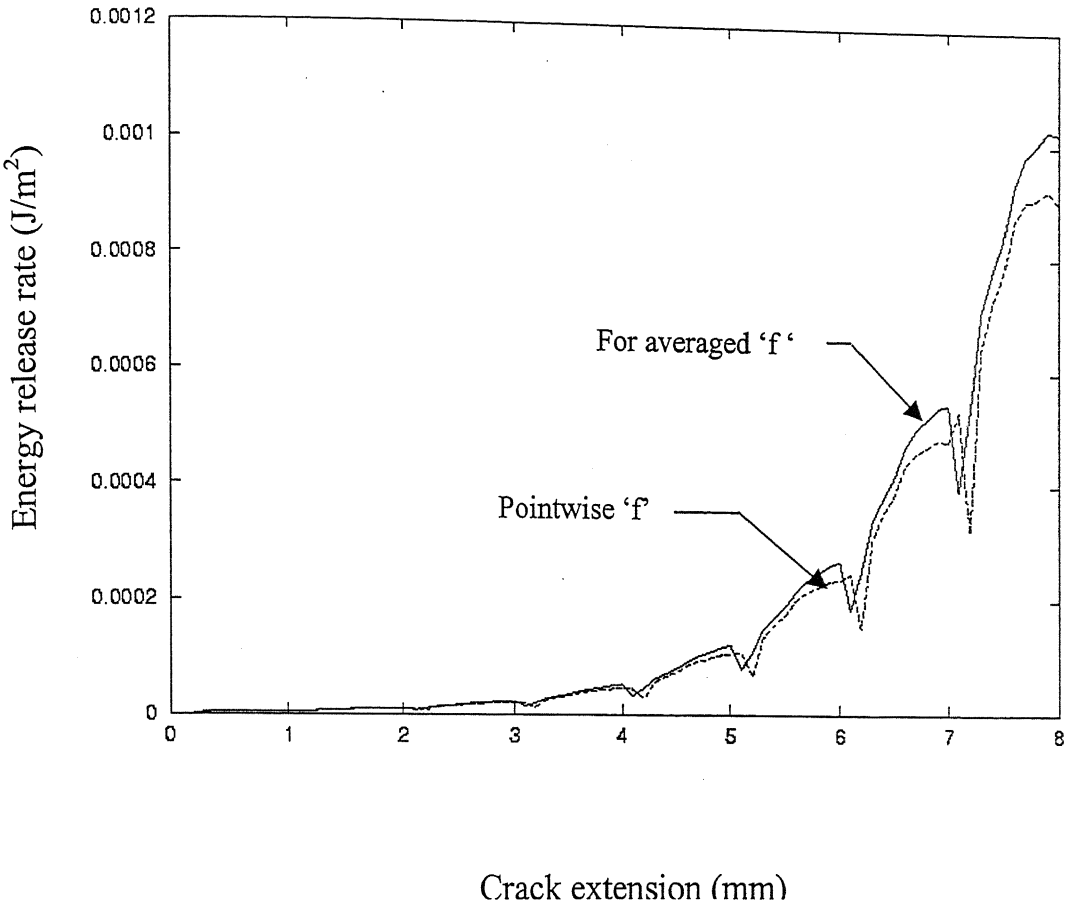

Fig 4.7 Effect of averaging 'f' values on energy release rate

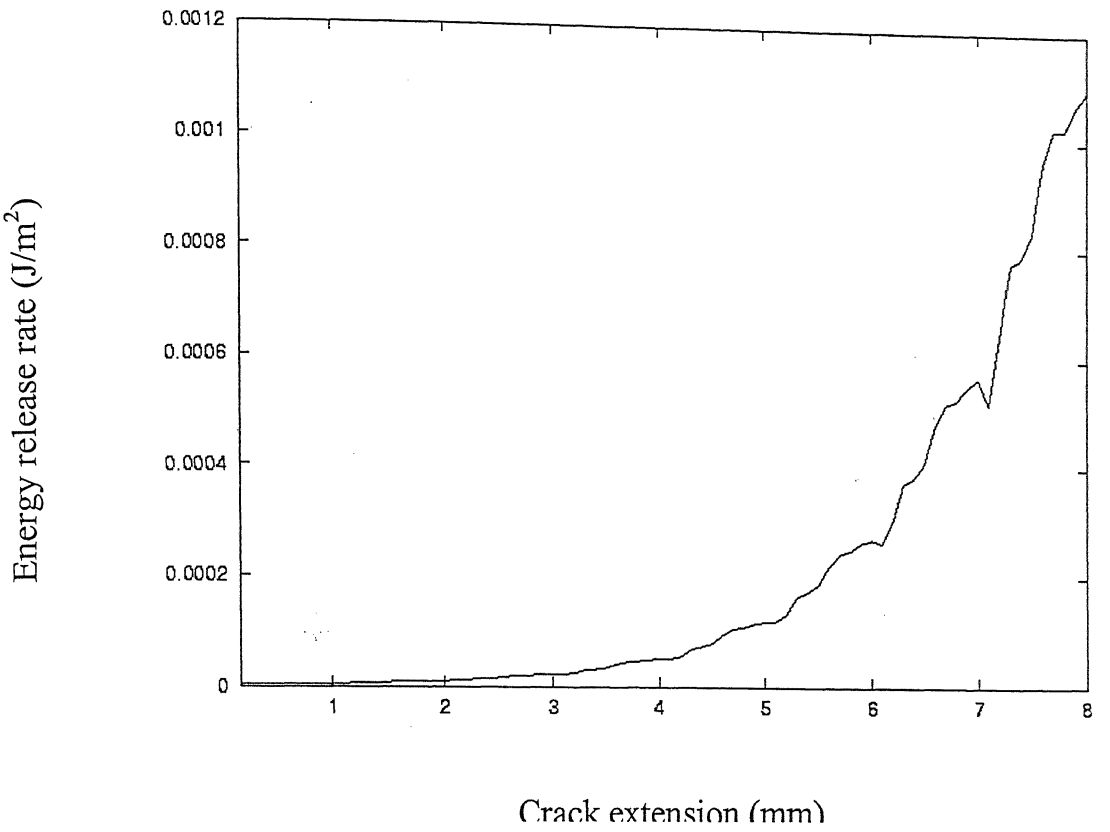

Fig 4.8 Energy release rate after shape function modification of elemental mass matrix

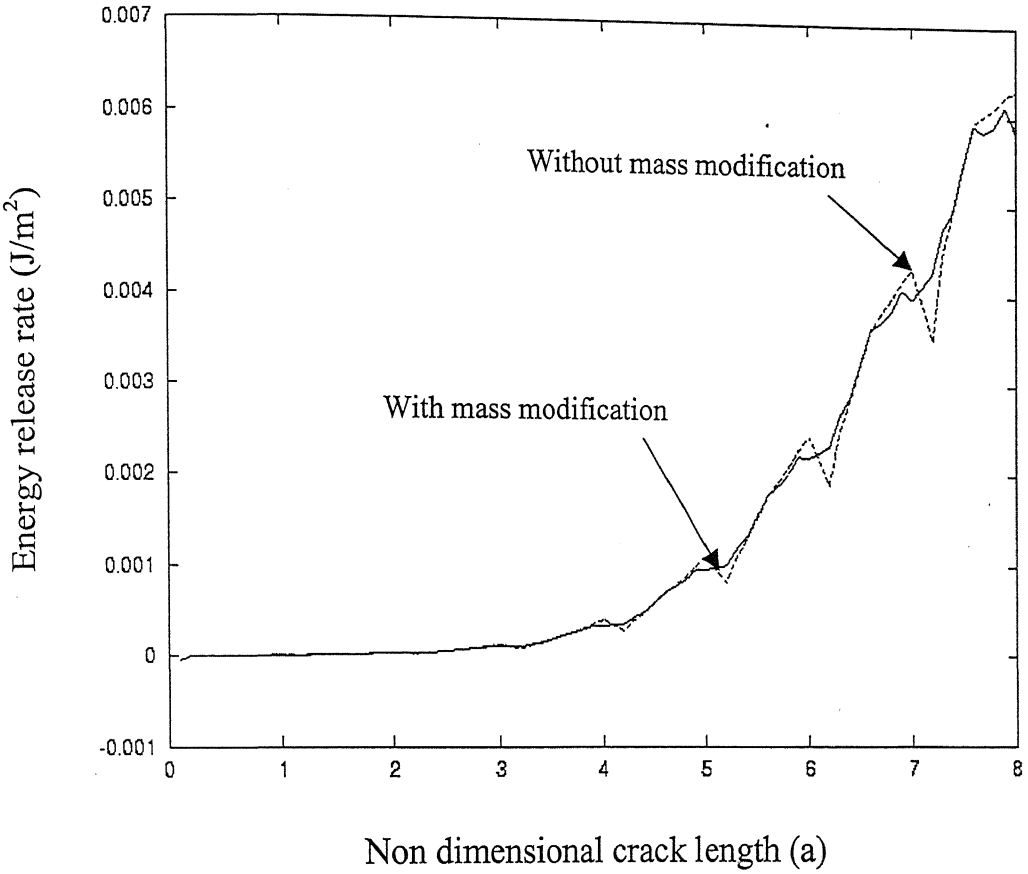

Fig 4.9 Energy release rate for crack velocity 1250m/s

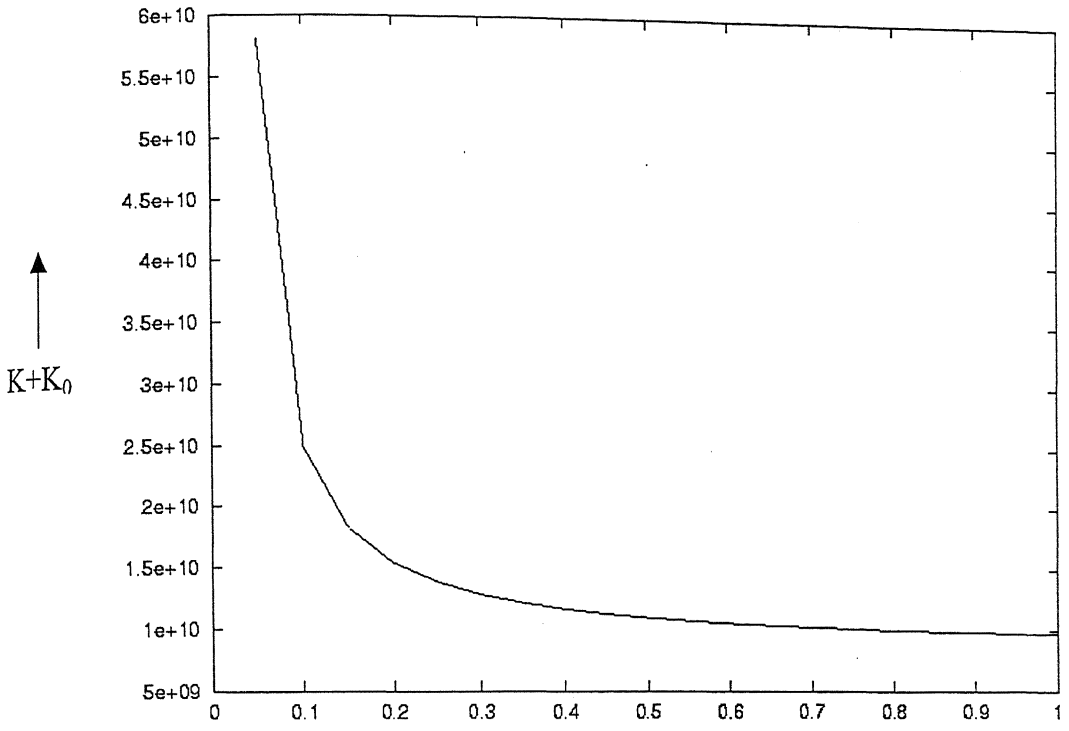

Fig 4.10 Effective stiffness at crack tip Vs 'a' without shape function modification

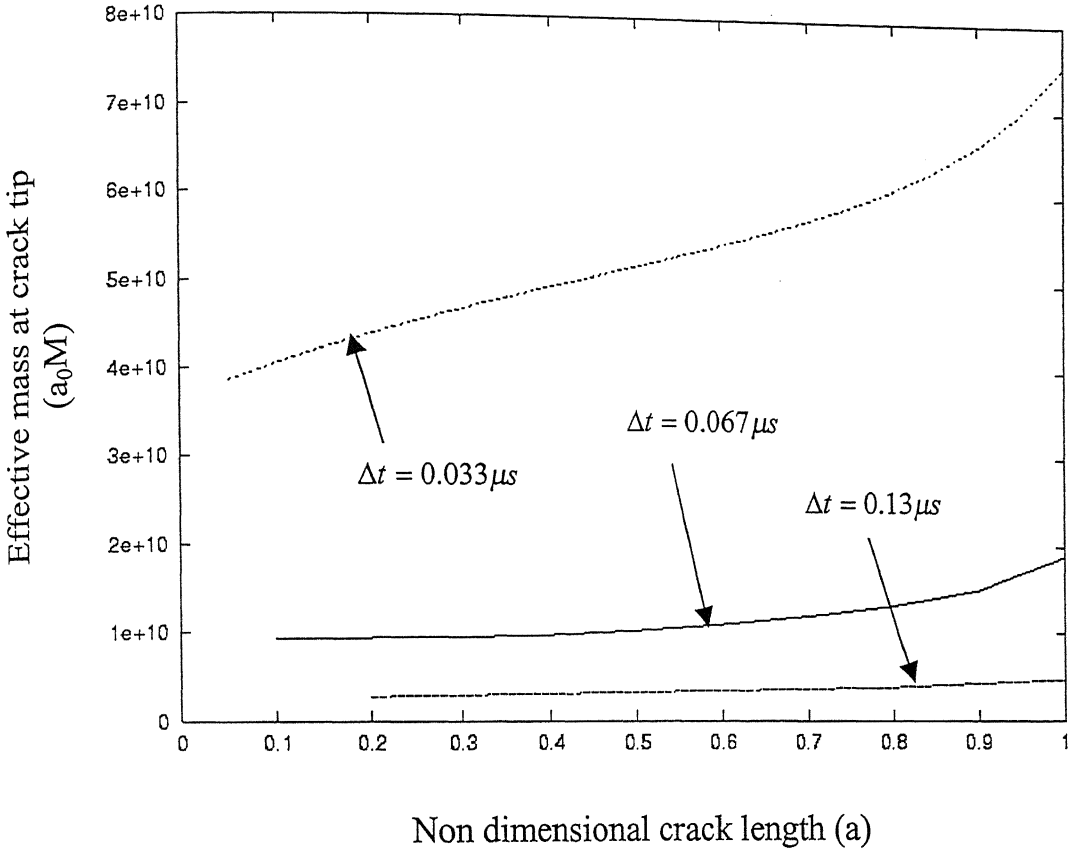

Fig 4.11 Variation of effective mass at crack tip Vs 'a'

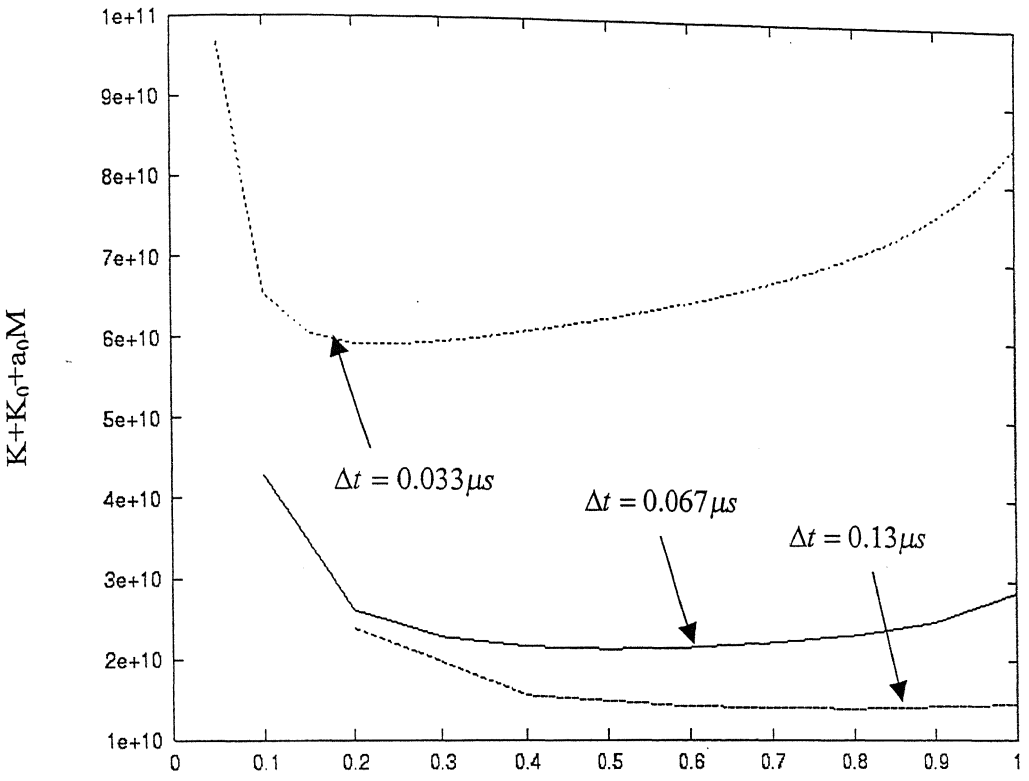

Fig 4.12 Variation of effective stiffness at crack tip Vs 'a'

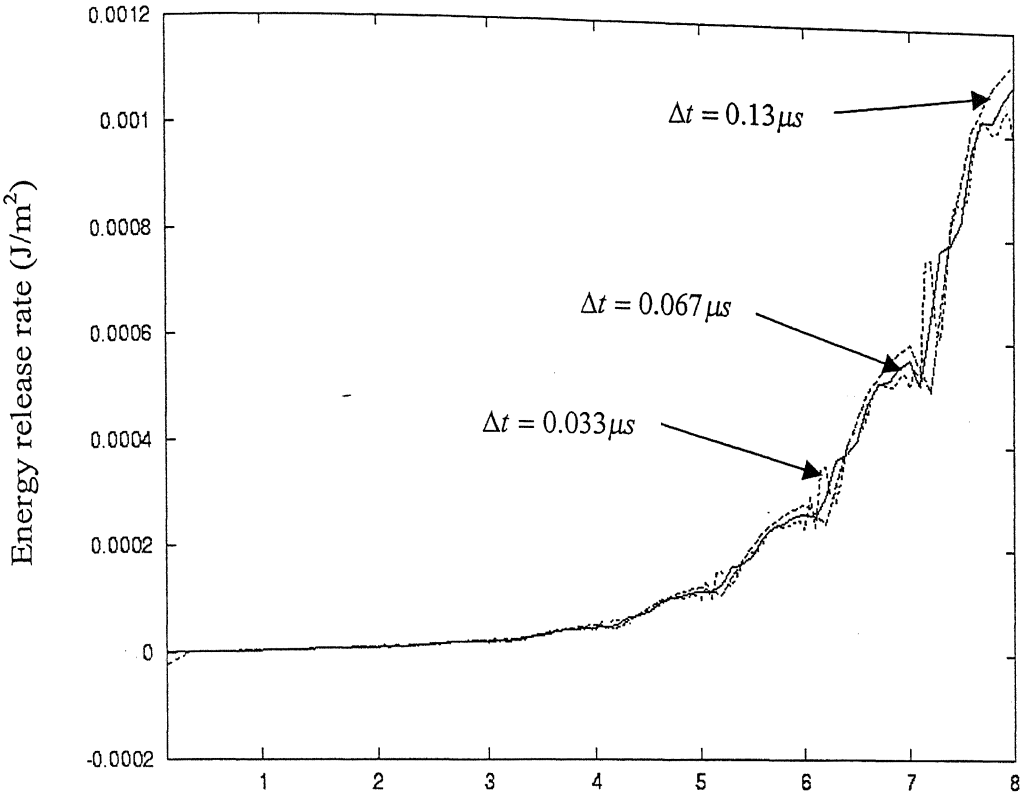

Fig 4.13 Energy release rate for different time steps

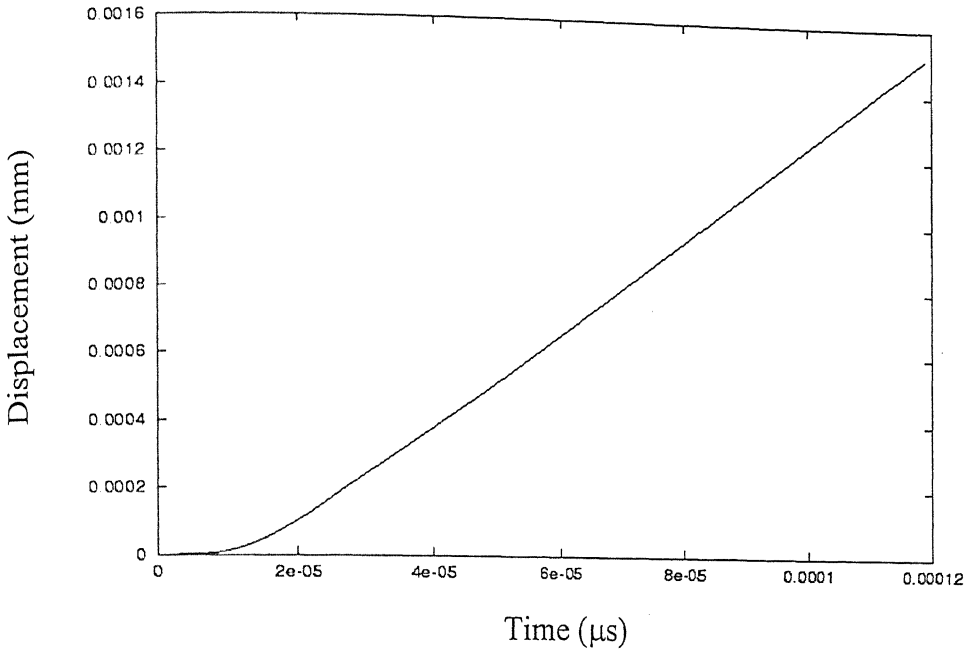

Displacement of the cantilever end (Expt 1)

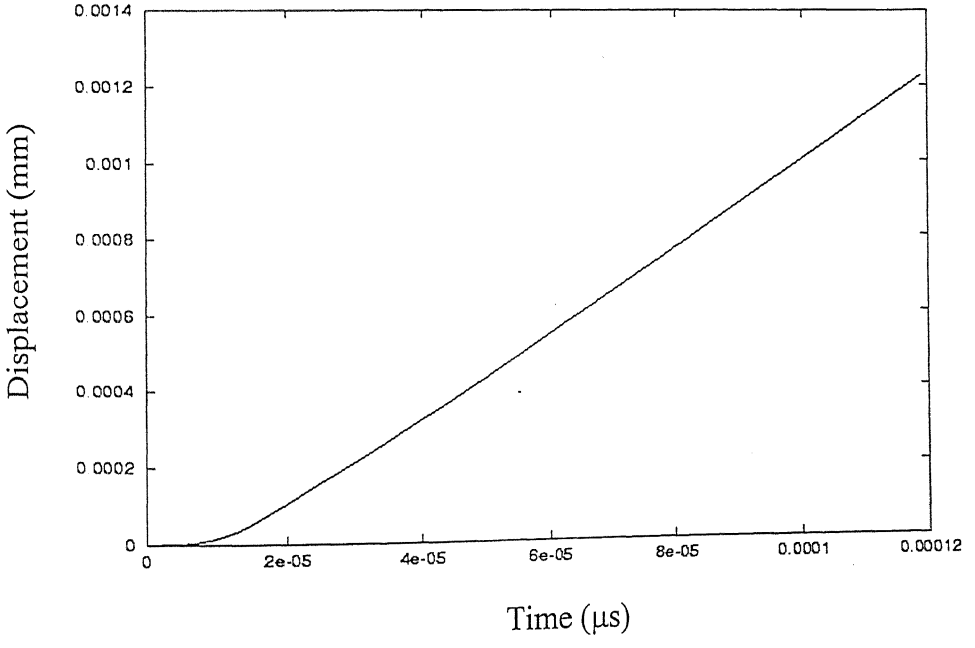

Displacement of the cantilever end (Expt 2)

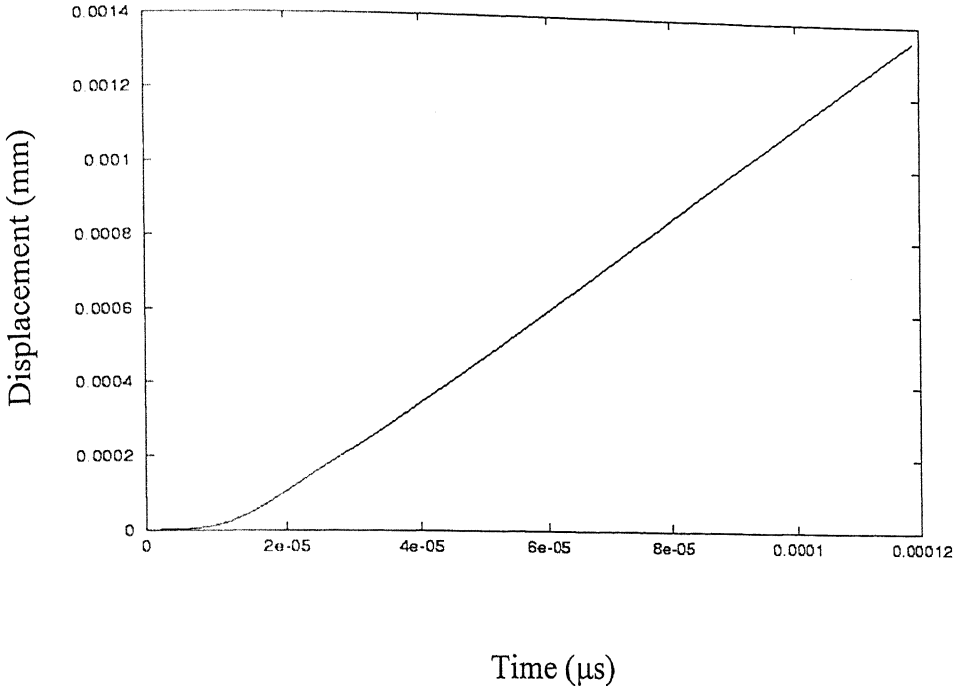

Displacement of the cantilever end (Expt 3)

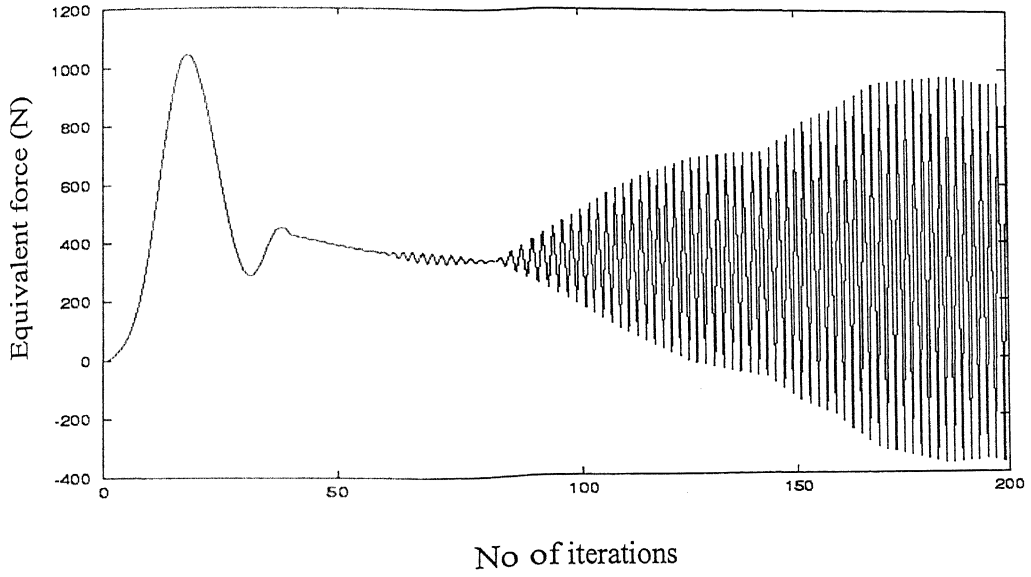

Resultant force using Newmark's method

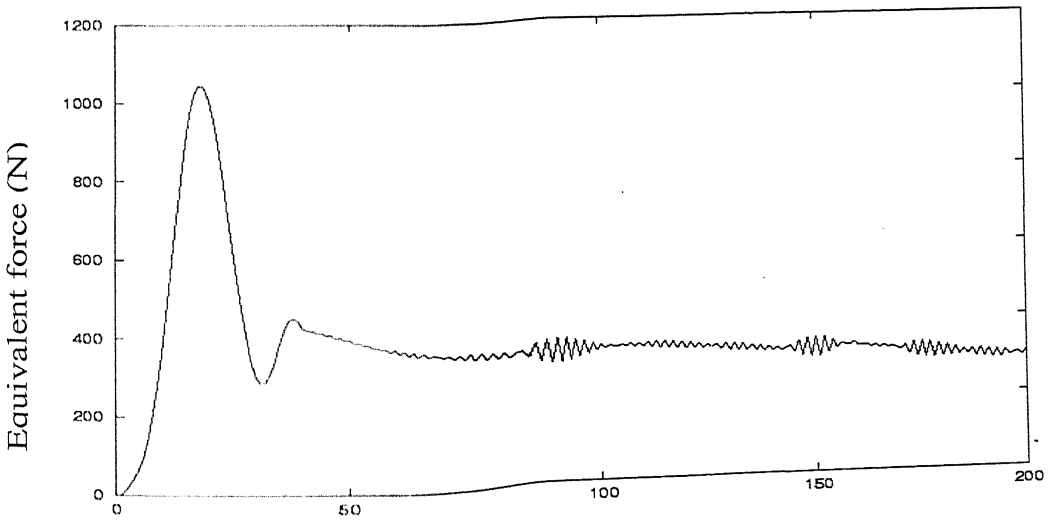

Resultant force using Theta method

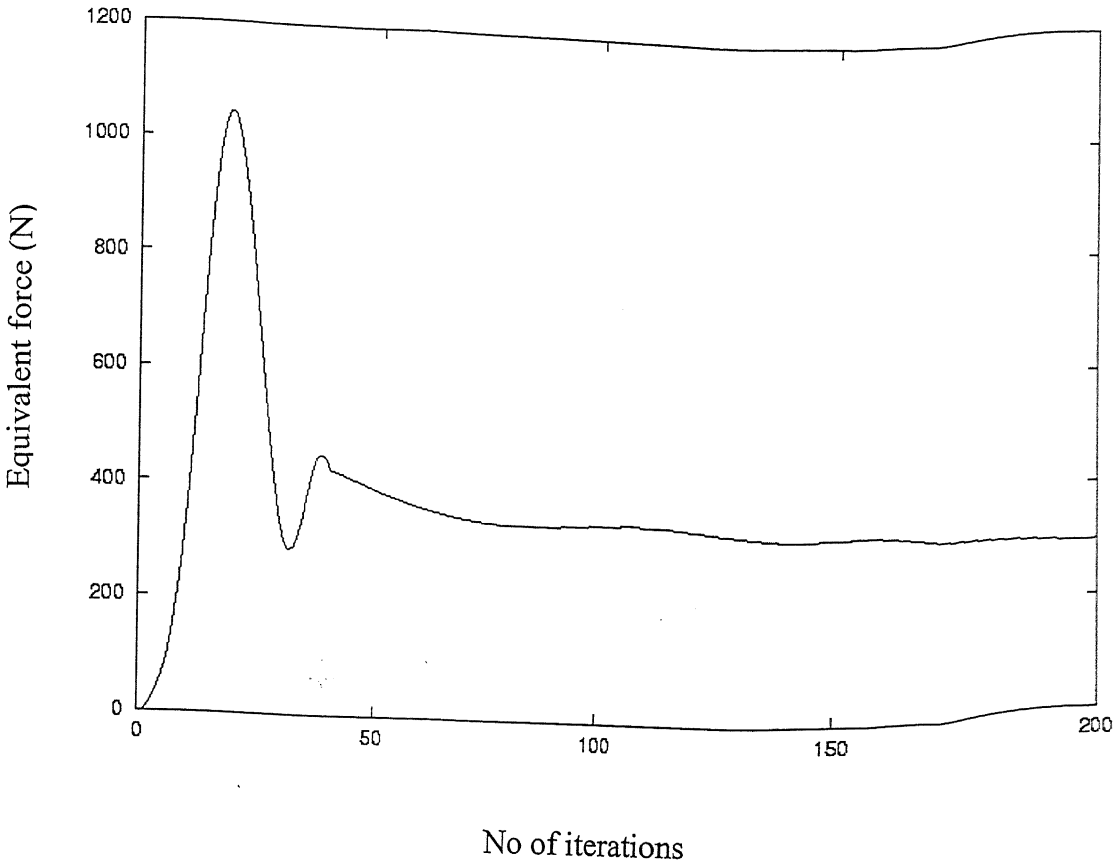

Resultant force after smoothening by Bezier curve

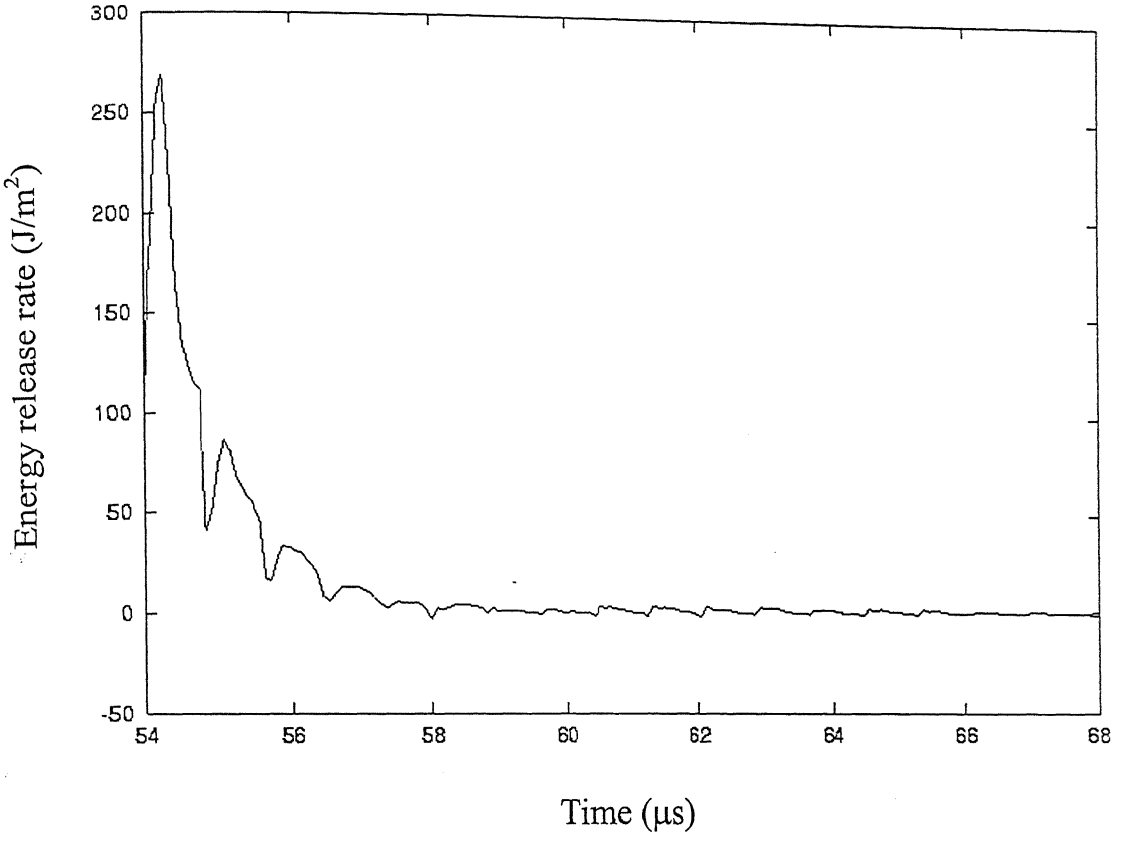

Fig 4.20 Energy release rate for Expt 1 (Present study)

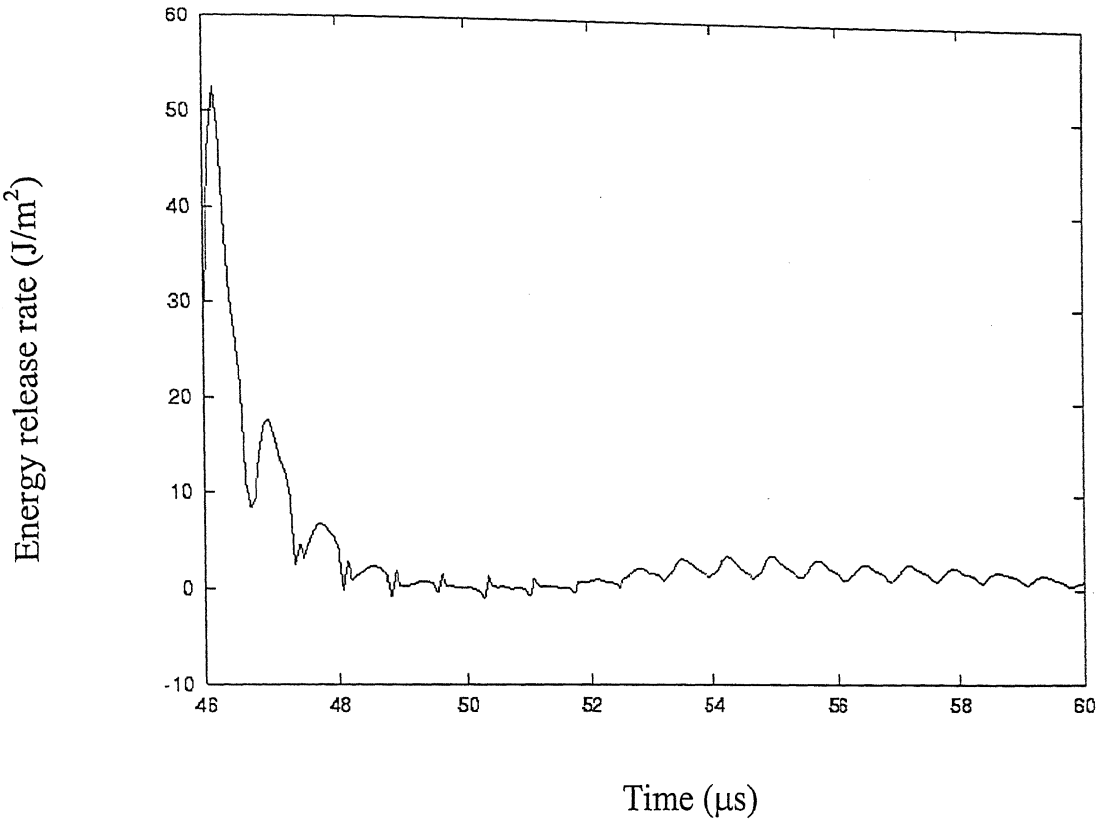

Fig 4.21 Energy release rate for Expt 2 (Present study)

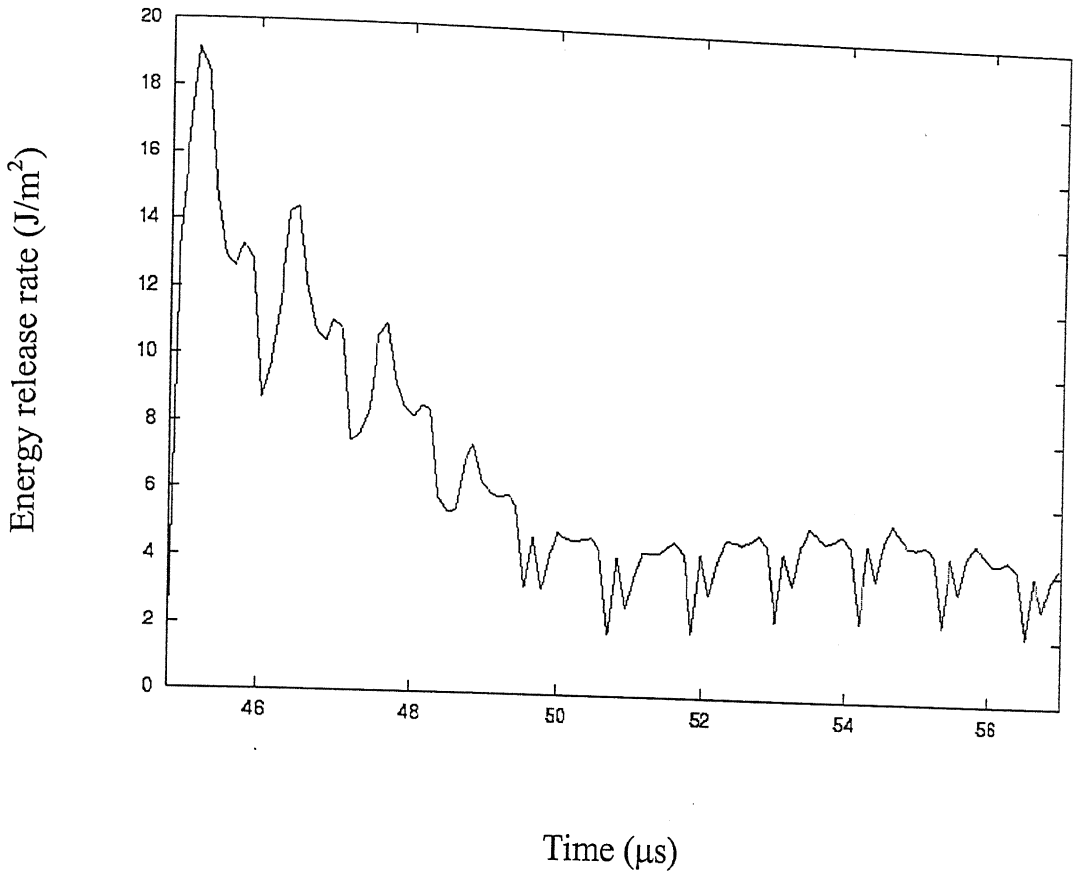

Fig 4.22 Energy release rate for Expt 3 (Present study)

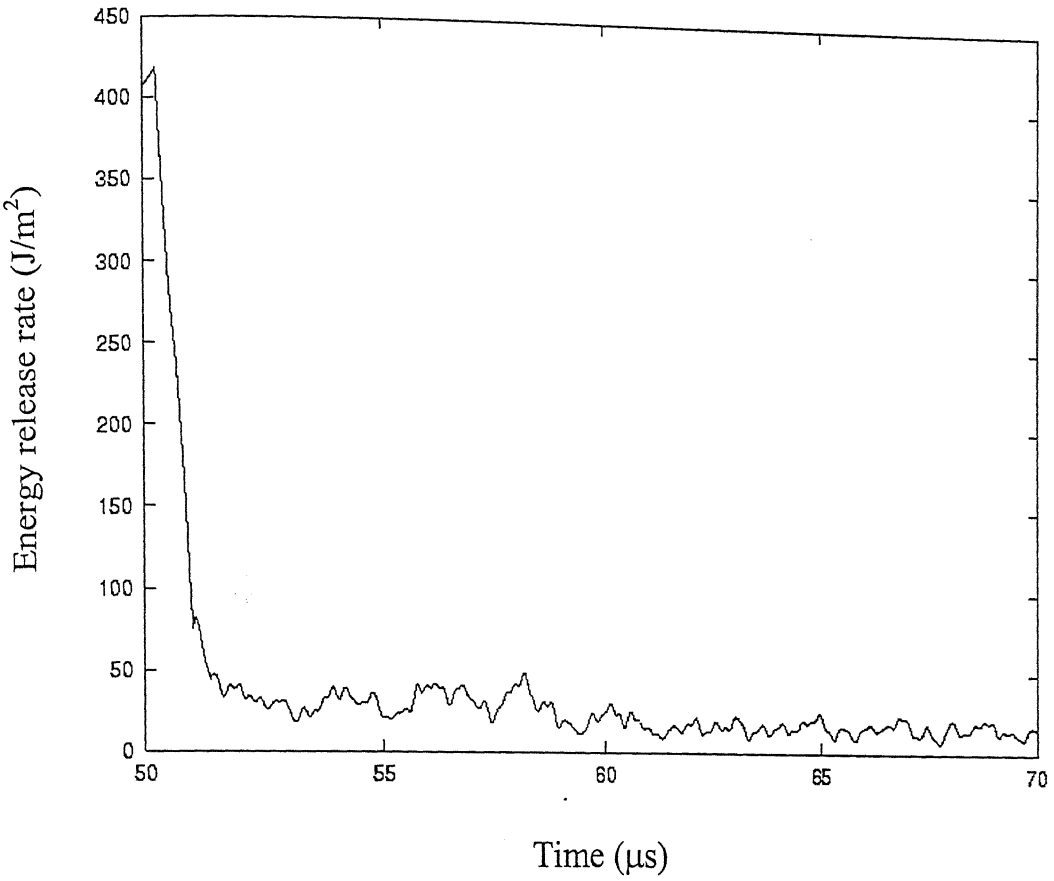

Fig 4.23 Energy release rate for Expt 1 by Force release model [27]

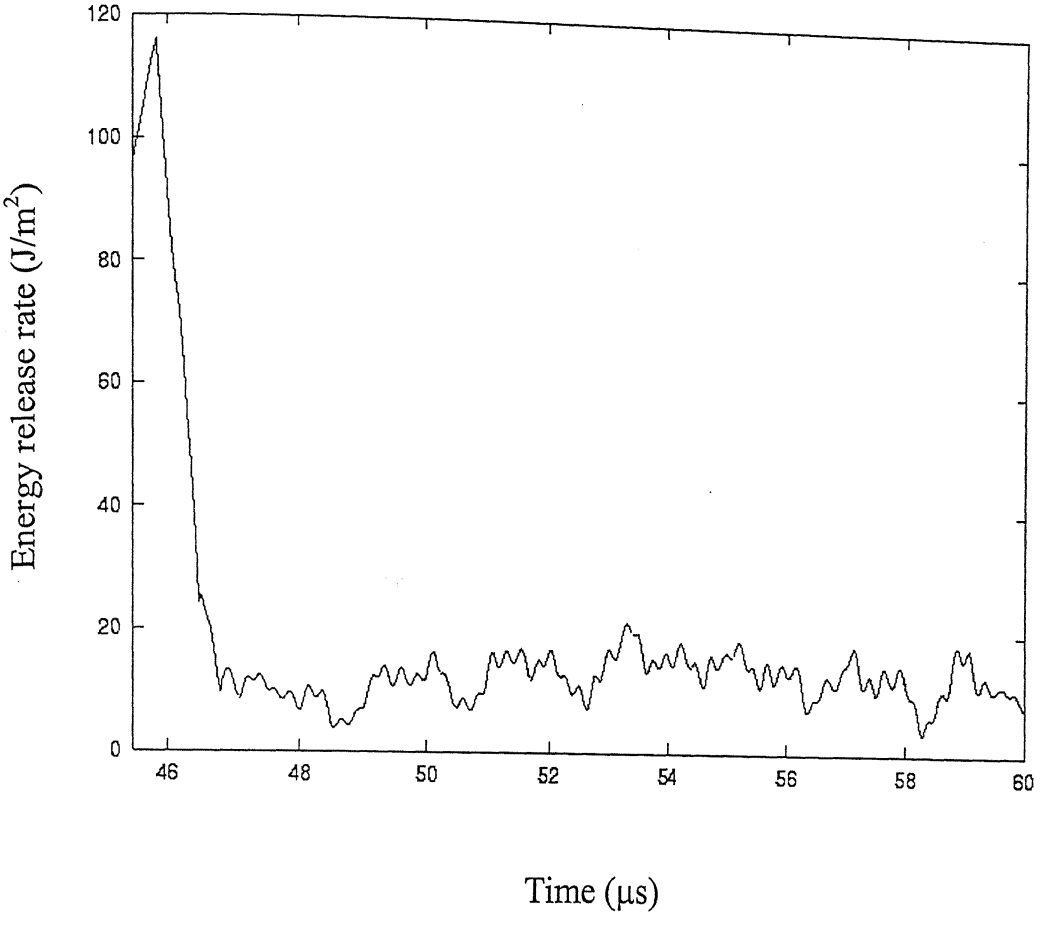

Fig 4.24 Energy release rate for Expt 2 by Force release model [27]

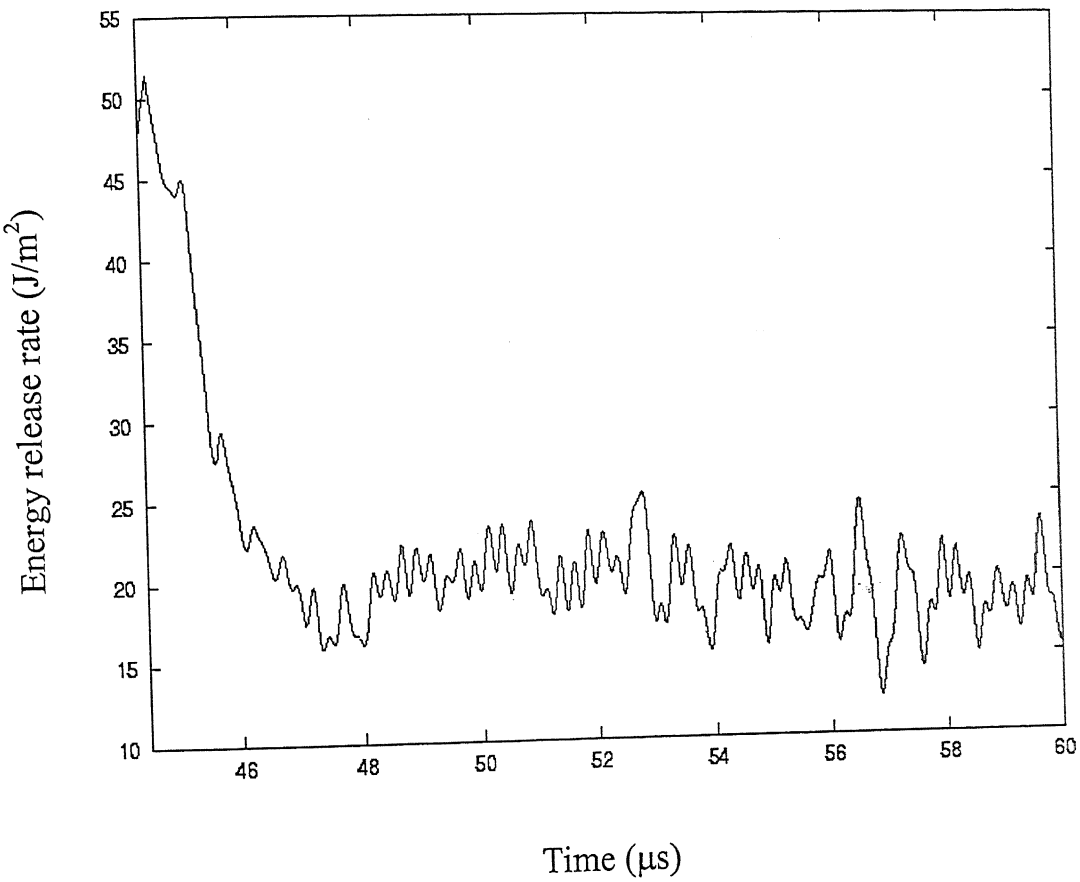

Fig 4.25 Energy release rate for Expt 3 by Force release model [27]

CHAPTER 5

CONCLUSIONS AND SCOPE FOR FUTURE WORK

5.1 Conclusions

A new model is proposed to investigate high speed crack propagation. This model involve further modification of stiffness release model and based on the results and discussion in Chap 4, following conclusions can be drawn.

1. Model gives fairly smooth and more stable variation of energy release rate.
2. Experimental results reveal that unlike force release model energy release rate doesn't drop to a low value in very few time steps but falls gradually which is a more practical result.
3. Out of two methods for solving equation of equilibrium (Newmark's and θ –method), θ –method was observed to be more stable.

5.2 Scope for Future Work

1. The crack propagation model may be further modified to get still better results.
2. Present method can be extended for Mode II and mixed mode crack propagation.
3. This method can also be extended for 3-Dimensional crack propagation problems.

REFERENCES

[1] Freund L. B., Dynamic Fracture Mechamics, Cambridge Univ. Press, Newyork, 1990

[2] Nishioka T. and Atluri S N., Computational Methods in Mechanics of Fracture,ed S. N. Atluri, Elsevier Science Publisher, Newyork, 1986

[3] Owen D R J and Shantaram D, Numerical study of dynamic crack growth by finite element method, Int. Journal of Fracture, vol 13, no 6,821-837,1977

[4] Nishioka T. and Atluri S N, Numerical analysis of dynamic crack propagation: Generation and prediction studies, Engg. Fracture Mechanics,**16,** 303-332,1982

[5] Nishioka T. and Atluri S N, Finite element simulation of fast fracture in steel DCB specimen, Engg. Fracture Mechanics,**16,** 157-175,1982

[6] Chaing C R, Determination of the dynamic stress intensity factor of a moving crack by numerical method, International Journal of Fracture,**45**,123-130,1990

[7] Thesken J C and Gudmundson Peter, Application of moving variable order singular element to dynamic fracture mechanics, Int. Journal of Fracture,**52**, 47-65,1991

[8] Kennedy T C and Kim J B, Dynamic analysis of cracks in micropolar elastic materials, Engg Fracture Mechanics,**27**, 227-298

[9] Wang Y and Williams J G, A numerical study of dynamic crack growth in isotropic DCB specimen, Composites, vol 25,no 5,323-331,1994

[10] Beissel S R, Johnson G R and Popelar C H, An element failure algorithm for dynamic crack propagation in general direction, Engg Fracture Mechanics,**61**, 407-425,1998

[11] Lin X B and Smith R A, Improved numerical technique for simulating the growth of a planer fatigue crack, Fatigue and Fracture of Engg materials and Structures,**20**,1363-1373,1997

[12] Siva Reddy, An FE model to investigate high speed crack propagation, MTech thesis, Mechanical Engg, IIT Kanpur,1997

[13] Bathe, Finite Element Procedure in Engg Analysis, Prentice Hall of India

[14] Hoff C and Phal PJ, Development of an implicit method with numerical dissipation from a generalised single-step algorithm for structural dynamics, Computer meth Appl Mech Engng ,**67**,367-385,1986

[15] Keegstra P N R, A transient finite element crack propagation model for nuclear pressure vessel steels, J. Inst. Nucl. Engrs,**17**,no 4,89-96,1976

[16] Keegstra P N R, Head J L and Turner C E, A two dimensional dynamic linear-elastic finite element program for the analysis of unstable crack propagation and arrest, Numerical methods in fracture mechanics, Eds. A R Luxmoore and D R J Owen (Univ. College, Swansea),634-47,1978

[17] Malluck J F and King W W, Fast fracture simulated by finite-element analysis which accounts for crack-tip energy dissipation, Numerical methods in fracture mechanics, Eds. A R Luxmoore and D J Owen (Univ. College,Swansea) 648-59,1978

[18] Rydholm G, Fredriksson B and Nilsson, Numerical investigation of rapid crack propagation, Numerical methods in fracture mechanics, Eds. A R Luxmoore and D J Owen (Univ. College,Swansea) 660-72,1978

[19] Kobayashi A S, Mall S, Urabe Y and Emery A F, A numerical dynamic fracture analysis of three wedge-loaded DCB specimens, Numerical methods in fracture mechanics, Eds. A R Luxmoore and D J Owen (Univ. College,Swansea) 673-84,1978

[20] Kishore N N, Kumar Prashant and Verma S K, Numerical Methods in Dynamic Fracture, Journal of Aeronautical Society of India, vol 45, no 4,323-333,1993.

[21] Aberson J A, Anderson J M and King W W, Singularity-element simulation of crack propagation, Fast fracture and crack arrest, Eds G T Hahn and M F Kannien, ASTM STP 627,123-34,1977

[22] Aberson J A, Anderson J M and King W W, Dynamic analysis of cracked structure using singularity finite elements, in Elasodynamic crack problems, Ed G C Sih (Noordhoff, Leyden),249-94,1977

[23] Williams M L, On stress distribution at the base of a singularity crack, J Appl Mech,**24**,109-14,1957

[24] Patterson C and Oldale M C, Analysis of an unstable crack growth and arrest problem using finite elements, Stability Problems in engg structures and cmponents, Eds T H Richards and P Stanley (Applied science publishers),281-96,1979

[25] Patterson C and Oldale M C, An analysis of fast fracture and arrest in DCB specimen using crack tip elements, Advances in fracture research,**5**,ICF5,2225-32,1981

[26] Griffith A A, The phenomenon of rupture and flow in solids, Philosophical transaction of the royal society (London) A211,163-98,1920

[27] Chudhary H, Dynamic interlaminar toughness of glass fabric/epoxy laminates, MTech thesis, Mechanical engg, IIT Kanpur,2000

[28] Agarwal B D and Broutman L J, Analysis and performance of fibre composites, 2nd ed, John Willey Sons, Inc,1990